RCS computations for realistic geometries – Issues & Challenges

Avijit Chatterjee

Department of Aerospace Engineering
Indian Institute of Technology, Bombay
Mumbai 400076, INDIA

Choice of a numerical solver

- Design stage (conceptual/ preliminary/ detailed)
- Fidelity (asymptotic PO, GTD, PTD / full wave MOM, FDTD, FVTD)
- Band requirement (VHF ……S……K,Ku)
- CPU time (min. …..days)
- Frequency / Time Domain
- Broadband/ single frequency
- Geometric complexity
- Material modeling
- Validation status
- Commercial / in-house

Maxwell Equation (differential form)

- Maxwell's curl Equations with losses:

$$\frac{\partial \mathbf{B}}{\partial t} = -\nabla \times \mathbf{E} - \rho \mathbf{H}$$

$$\frac{\partial \mathbf{D}}{\partial t} = \nabla \times \mathbf{H} - \mathbf{J}_i - \sigma \mathbf{E}$$

- Constitutive Relations

$$\mathbf{D} = \varepsilon' \mathbf{E}$$
$$\mathbf{B} = \mu' \mathbf{H}$$
$$\sigma = \omega \varepsilon''$$
$$\rho = \omega \mu''$$

$$\varepsilon_r = \varepsilon' - j\varepsilon''$$
$$\mu_r = \mu' - j\mu''$$

Finite Volume Time Domain solver

- Full wave in time domain
- No assumptions
- Deals with complex geometries
- Structured/ unstructured
- Material (dielectric/ lossy/ dispersive)
- Validations
- In-house code for many defence applications

Motivation

- Circa 1990: Well developed finite volume based capability for solving unsteady Euler equations of fluid dynamics….
- Idea to borrow expertise to solve Maxwell's equations in conservative form for EM scattering from aerospace configurations and predict Radar Cross Section (RCS) - Finite Volume Time Domain (FVTD) schemes….Vijayashankar et al. (1990).
- An "exact" technique able to deal with complex geometries, broadband signals and varying material properties.
- The major disadvantage is terms of CPU time because of fine mesh required (points per wavelength).

Maxwell Equation in Conservative form

3D Maxwell's Equations in Conservative form:

$$\mathbf{u}_t + \mathbf{f}(u)_x + \mathbf{g}(u)_y + \mathbf{h}(u)_z = \mathbf{s}$$

where,

$$u = \begin{pmatrix} B_x \\ B_y \\ B_z \\ D_x \\ D_y \\ D_z \end{pmatrix}; f = \begin{pmatrix} 0 \\ -D_z/\varepsilon' \\ D_y/\varepsilon' \\ 0 \\ B_z/\mu' \\ -B_y/\mu' \end{pmatrix}; g = \begin{pmatrix} D_z/\varepsilon' \\ 0 \\ -D_x/\varepsilon' \\ -B_z/\mu' \\ 0 \\ B_x/\mu' \end{pmatrix}; h = \begin{pmatrix} -D_y/\varepsilon' \\ D_x/\varepsilon' \\ 0 \\ B_y/\mu' \\ -B_x/\mu' \\ 0 \end{pmatrix}; s = \begin{pmatrix} -\rho H_x \\ -\rho H_y \\ -\rho H_z \\ -J_{ix} - \sigma E_x \\ -J_{iy} - \sigma E_y \\ -J_{iz} - \sigma E_z \end{pmatrix}$$

Numerical Formulation

- Maxwell's Equations (Operator form)

$$L(u) = s$$

- Decomposition of Total Field

$$L(u^i + u^s) = s^i + s^s$$

$$L(u^s) = s^s + S^i$$

$$S^i = -L(u^i) + s^i$$

Finite Volume Framework

- conservative form (scattered formulation) can be written as

$$\mathbf{u}_t^s + \mathbf{f}(\mathbf{u}^s)_x + \mathbf{g}(\mathbf{u}^s)_y + \mathbf{h}(\mathbf{u}^s)_z = \mathbf{s}^s + \mathbf{S}^i$$

where

$$\mathbf{S}^i = -\mathbf{u}_t^i - \mathbf{f}(\mathbf{u}^i)_x - \mathbf{g}(\mathbf{u}^i)_y - \mathbf{h}(\mathbf{u}^i)_z + \mathbf{s}^i$$

- integrating over an arbitrary control volume,

$$\frac{\partial \int_v \mathbf{u}^s dV}{\partial t} + \int_v \nabla \cdot [\mathbf{F}(\mathbf{u}^s)] dV$$

$$= \int_v (s^s + s^i) dV - \frac{\partial \int_v \mathbf{u}^i dV}{\partial t} - \int_v \nabla \cdot [\mathbf{F}(\mathbf{u}^i)] dV$$

Finite Volume Framework ….contd

application of divergence theorem gives,

$$\frac{\partial \int_v \mathbf{u}^s dV}{\partial t} + \int_s [\mathbf{F}(\mathbf{u}^s) + \mathbf{F}(\mathbf{u}^i)] \cdot \hat{n} dS = \int_v (s^s + s^i - u_t^i) dV$$

- 3D domain divided into hexahedral cells (structured mesh)
- Cell centred / vertex formulation

discretized form for jth cell,

$$V_j \frac{d\tilde{\mathbf{u}}_j^s}{dt} + \sum_{m=1}^{M} (\{[\mathbf{F}(\mathbf{u}^s) + \mathbf{F}(\mathbf{u}^i)] \cdot \hat{n} S\}_m)_j = V_j (\tilde{s}_j^s + \tilde{s}_j^i - \frac{d\tilde{\mathbf{u}}_j^i}{dt})$$

- Higher order characteristic based technique
- Runge Kutta time stepping

Boundary conditions, methodology

On Perfectly Conducting (PEC) surface:

- Total tangential electric field, $\mathbf{n} \times \mathbf{E} = 0.$
- Total normal magnetic field, $\mathbf{n} \cdot \mathbf{B} = 0.$

Far-field boundaries:

- Characteristic boundary conditions (zero scattered field) etc.

In time:

- ➢ *Time domain computations for sinusoidal steady state.*
- ➢ *Complex field in frequency domain from time history of solution using Fourier Transform.*
- ➢ *RCS requires computing scattered field at far-field. Obtained by calculating electric vector potential in the farfield based on complex currents on surface enclosing scatterer.*

Numerical schemes

Differ by how numerical flux f_{num} is evaluated at cell face and by how time integration is performed

- **Upwind (Characteristic based) Schemes:**

  Flux Splitting Schemes, Riemann/Godunov Solvers

- **Central Difference based Schemes:**

  Lax-Wendroff Scheme, Jameson's scheme

- **Space and Time discretization combined:**

  Lax Wendroff Scheme (Taylor series in time)

- **Space and Time seperated:**

  Set of ODE's obtained after space discretization
  March in time with Runge-Kutta method

Validation

Metallic sphere:

- Volume grid O-O Topology, Single Block (50×45×20 cells)
- Frequency for analysis = 0.09 GHz (Electric Size = 1.4660)

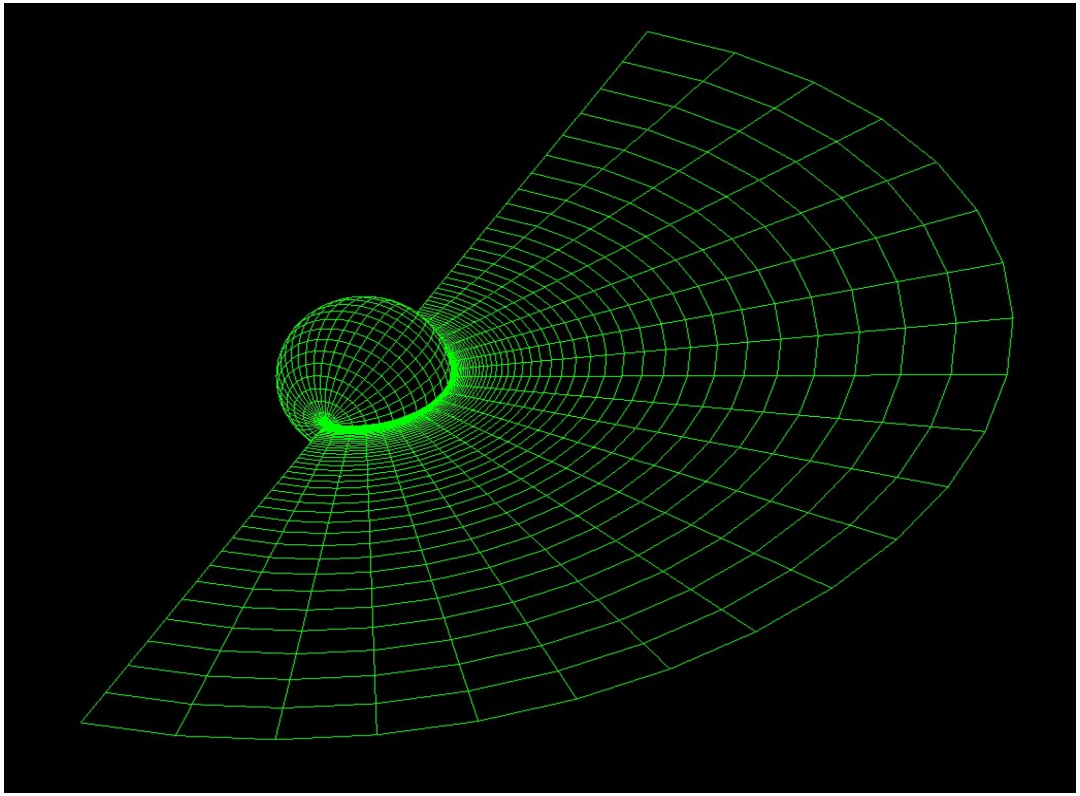

Volume grid discretization (O-O Topology)

Validation ….contd

Metallic Sphere:

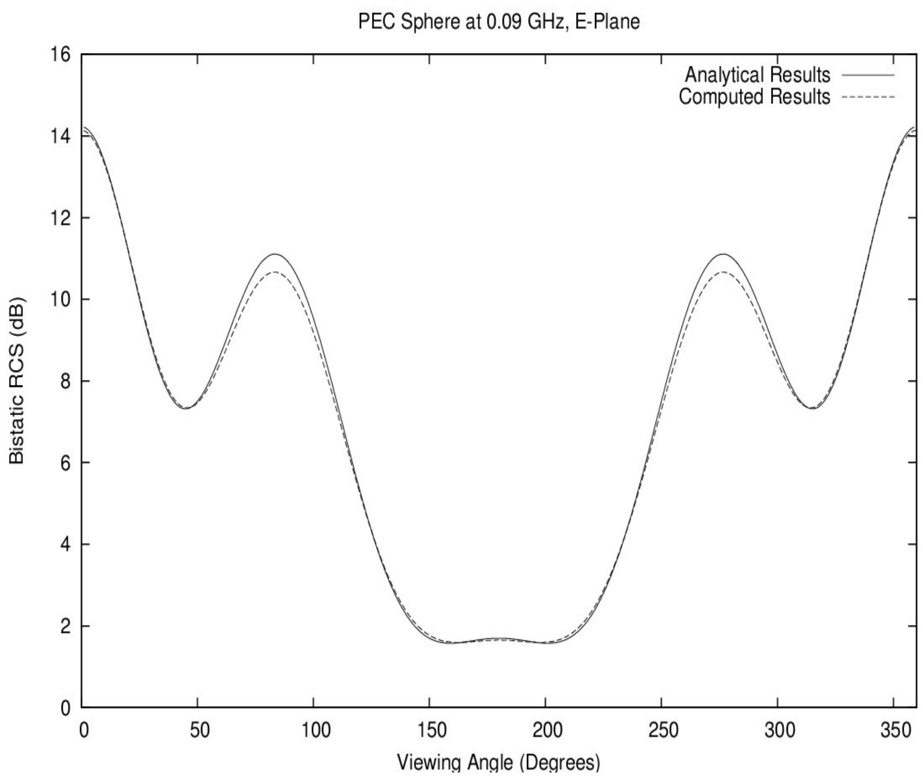

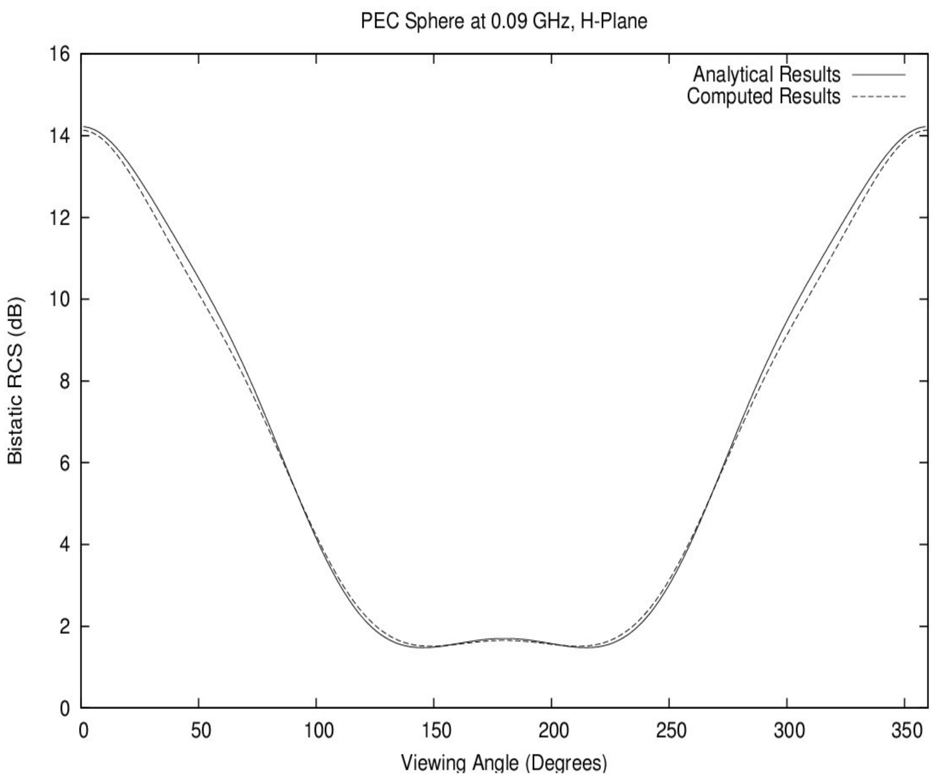

E-plane **H-plane**

Bistatic RCS (dB) for Metallic Sphere at 0.09 GHz

Validation

Metallic Ogive: (EMCC benchmark)

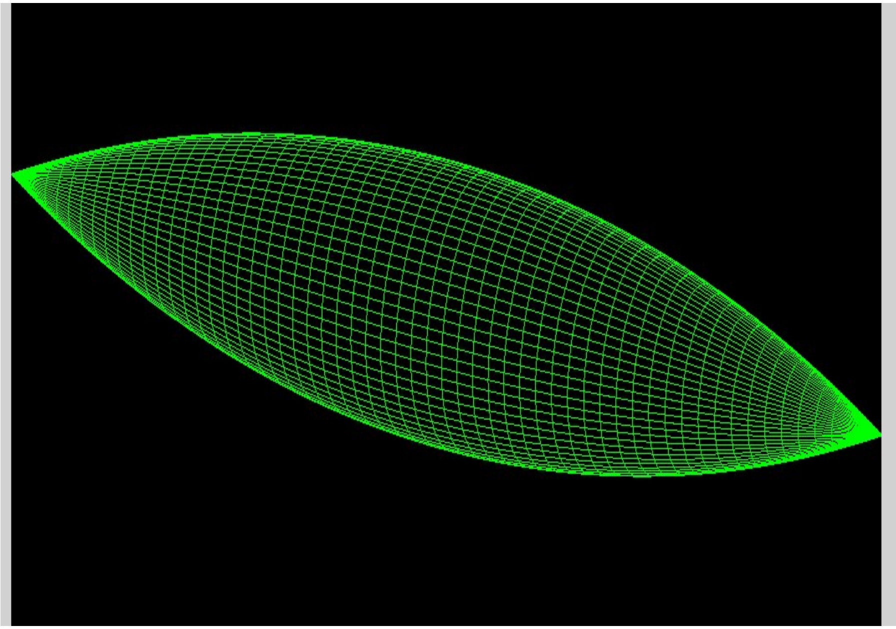

Surface grid

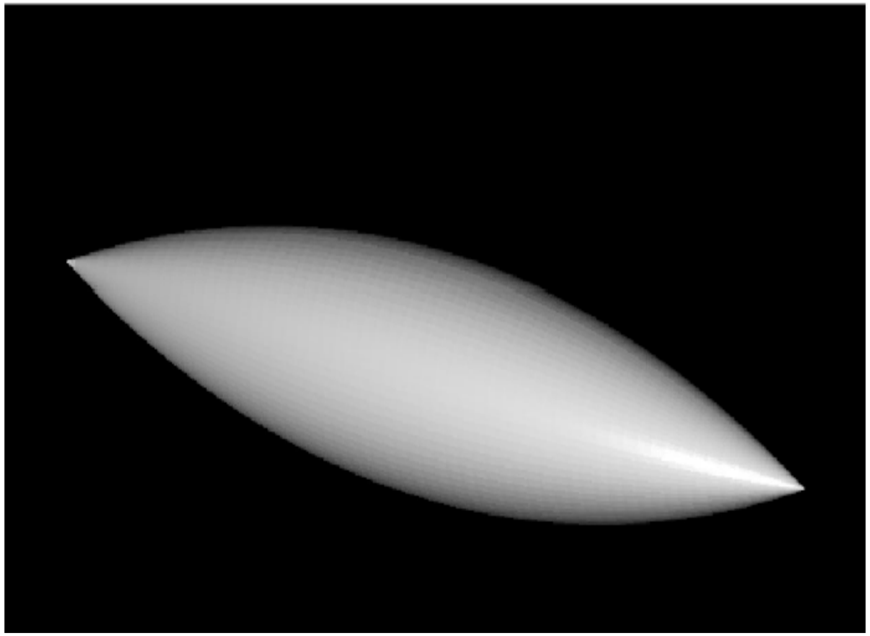

Rendered ogive

Validation ….contd

Metallic ogive:

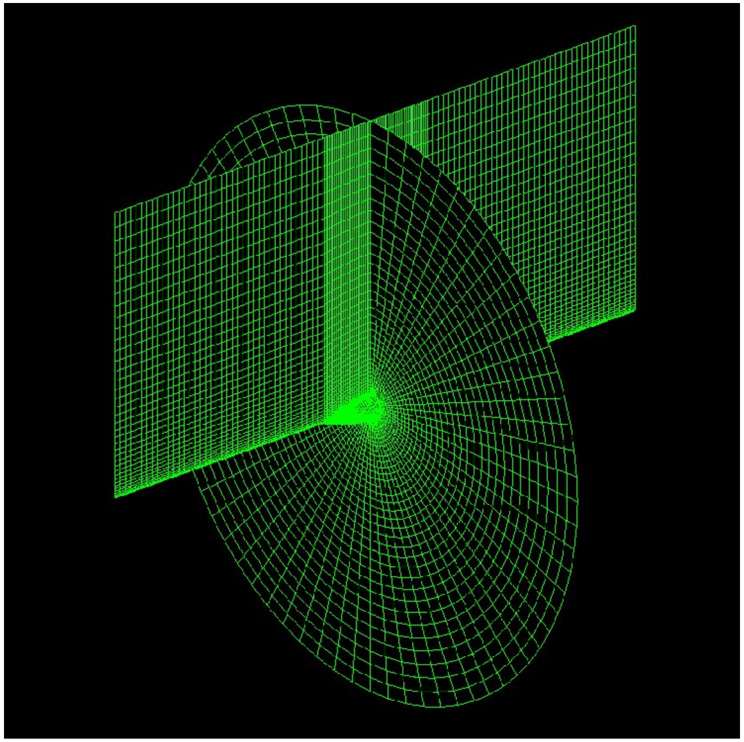

Ogive Volume Grid Cross-Section

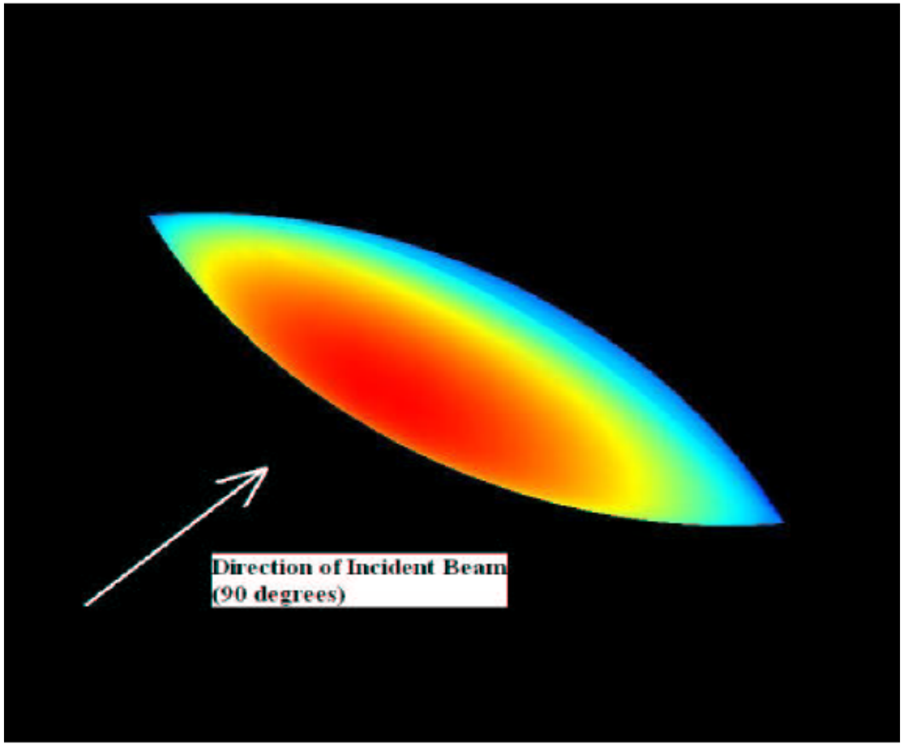

(Surface currents on the ogive at 90 degrees incidence)

Ogive – volume grid and surface currents

Validation ….contd

Metallic Ogive:

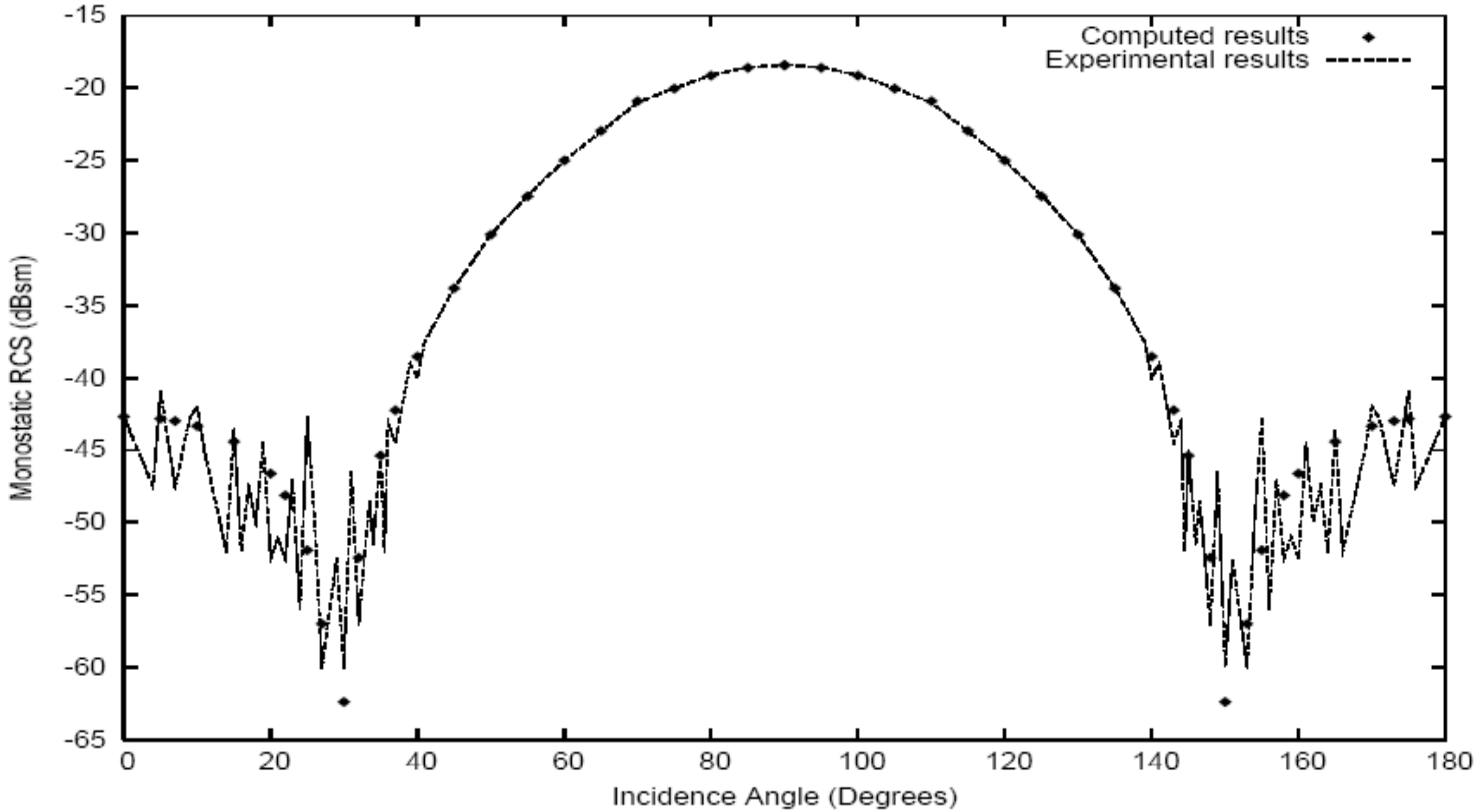

Ogive monostatic RCS Plot (1.18 GHz, VV Polarization)

Engine intakes

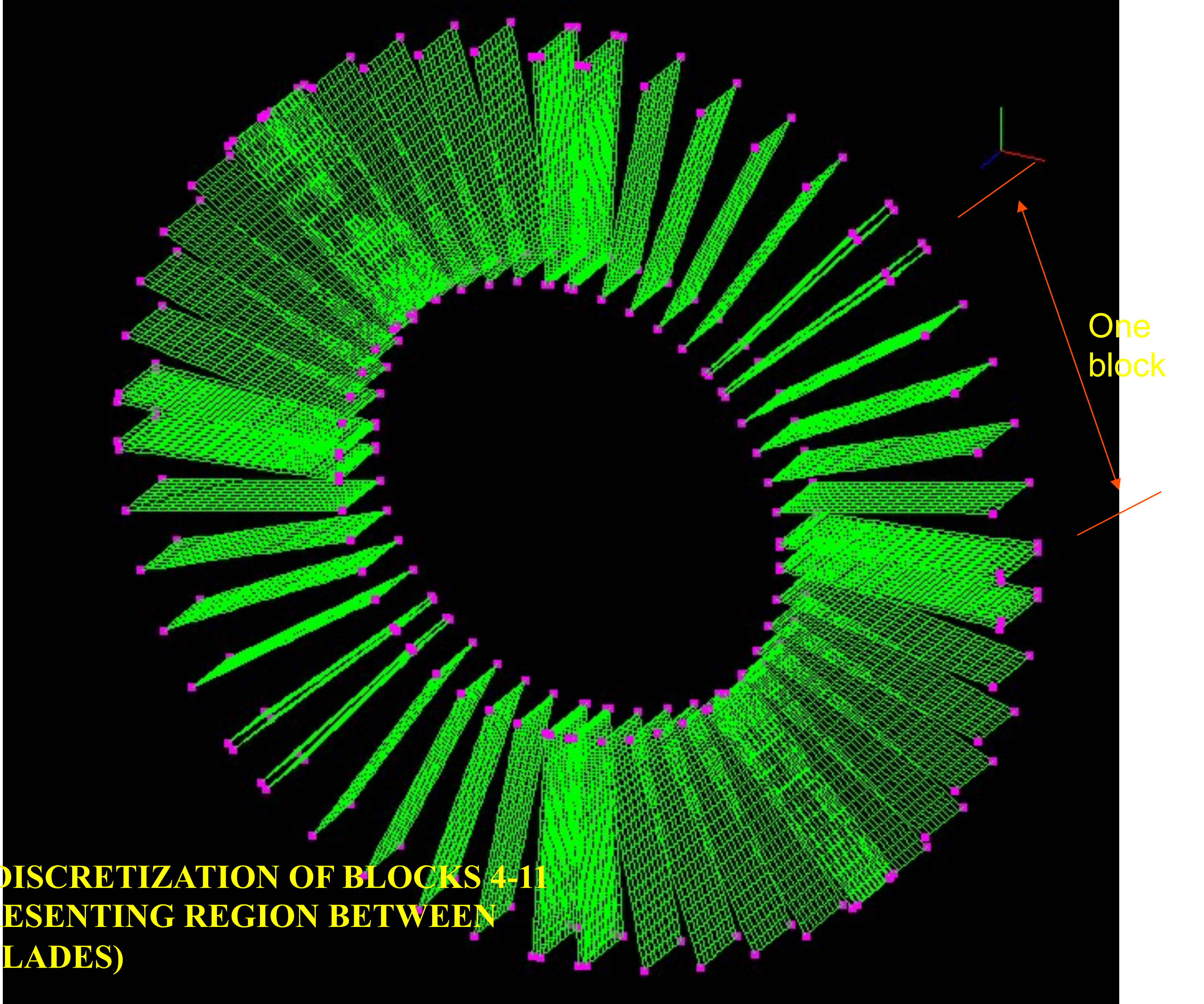

VOL. DISCRETIZATION OF BLOCKS 4-11
(REPRESENTING REGION BETWEEN
THE BLADES)

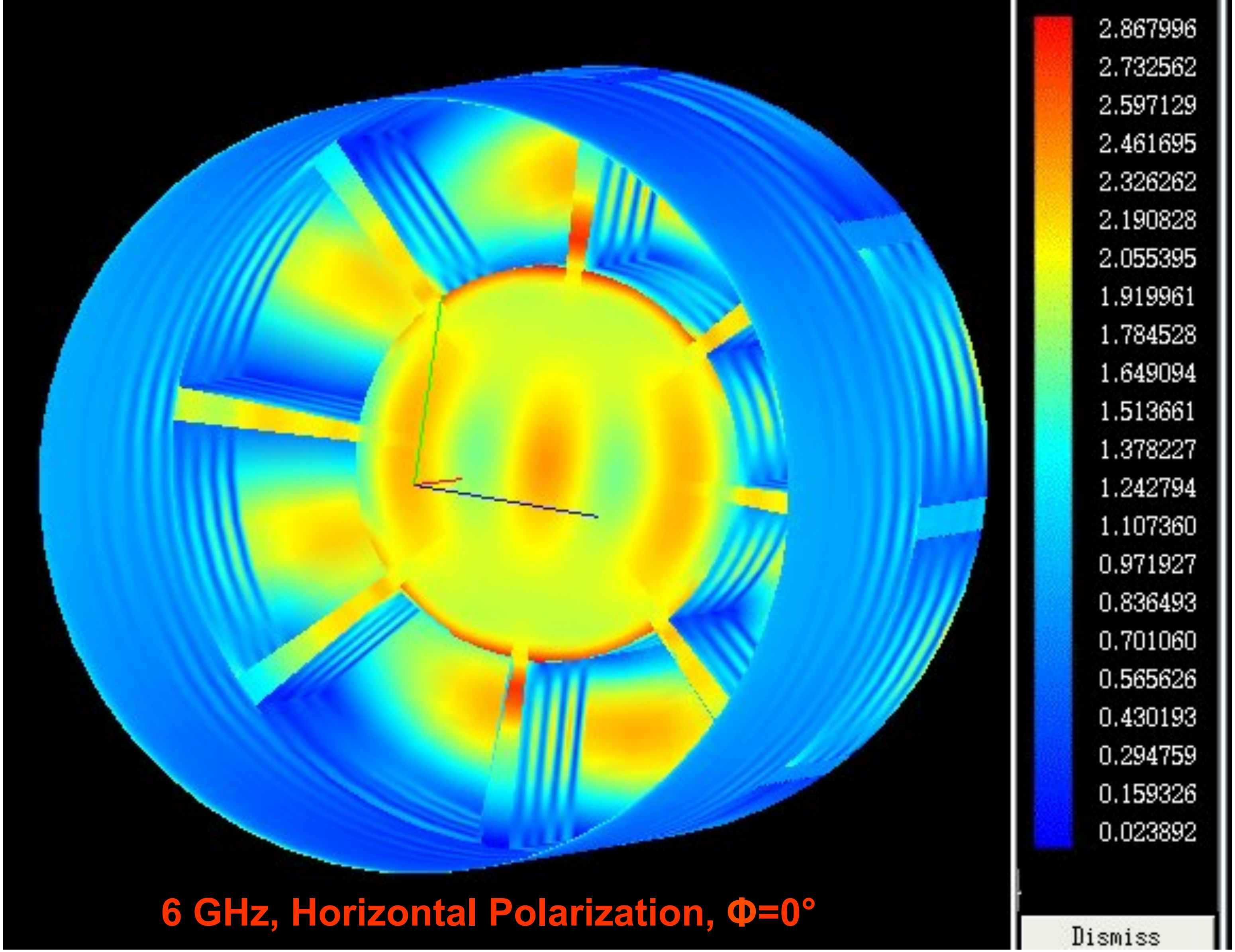

Surface Current Distribution on Straight Cylindrical Cavity with Hub, Blades and Plate terminations

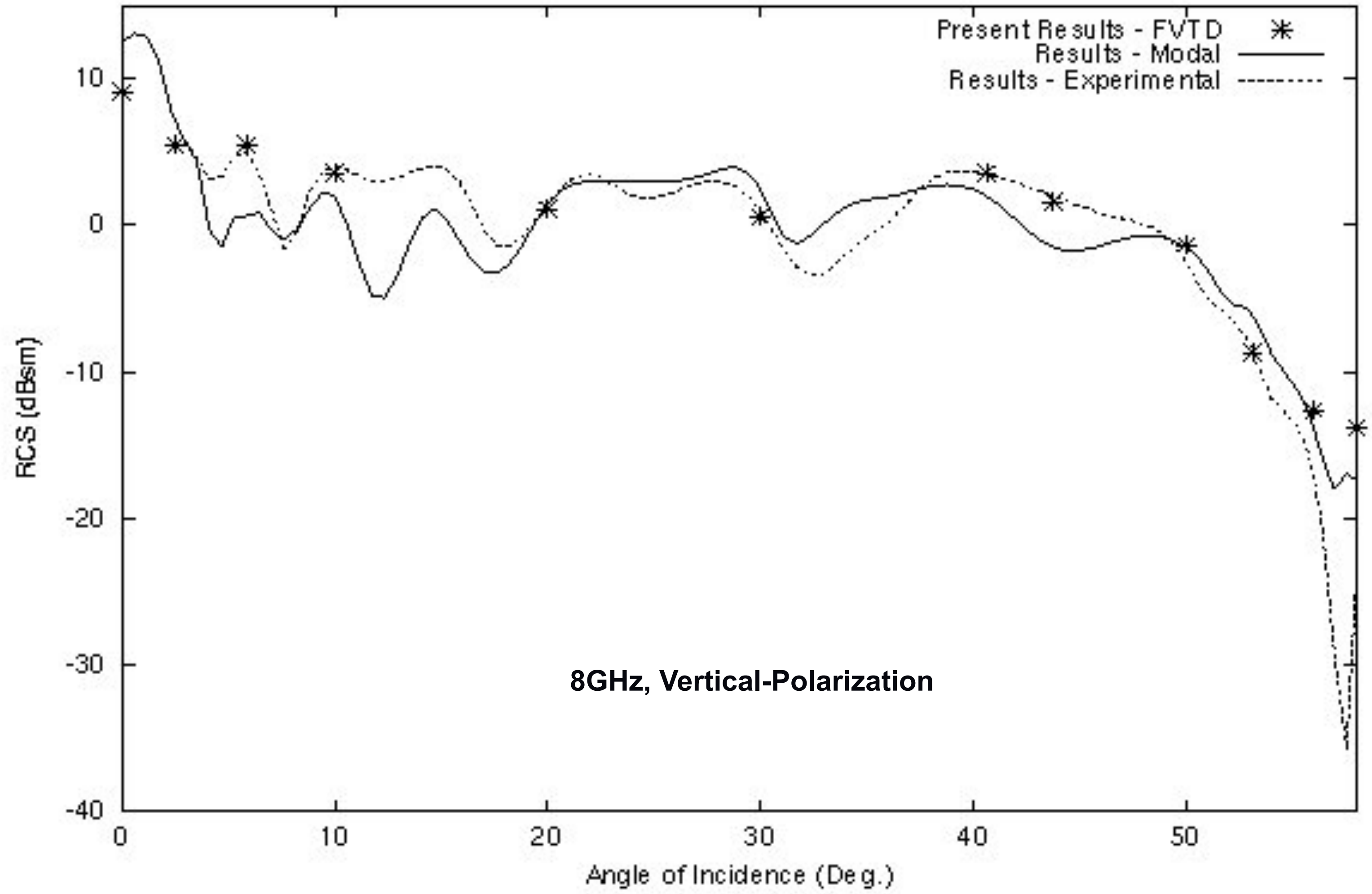

Monostatic RCS: Straight Cylindrical Cavity with a Hub, Blades and Plate termination

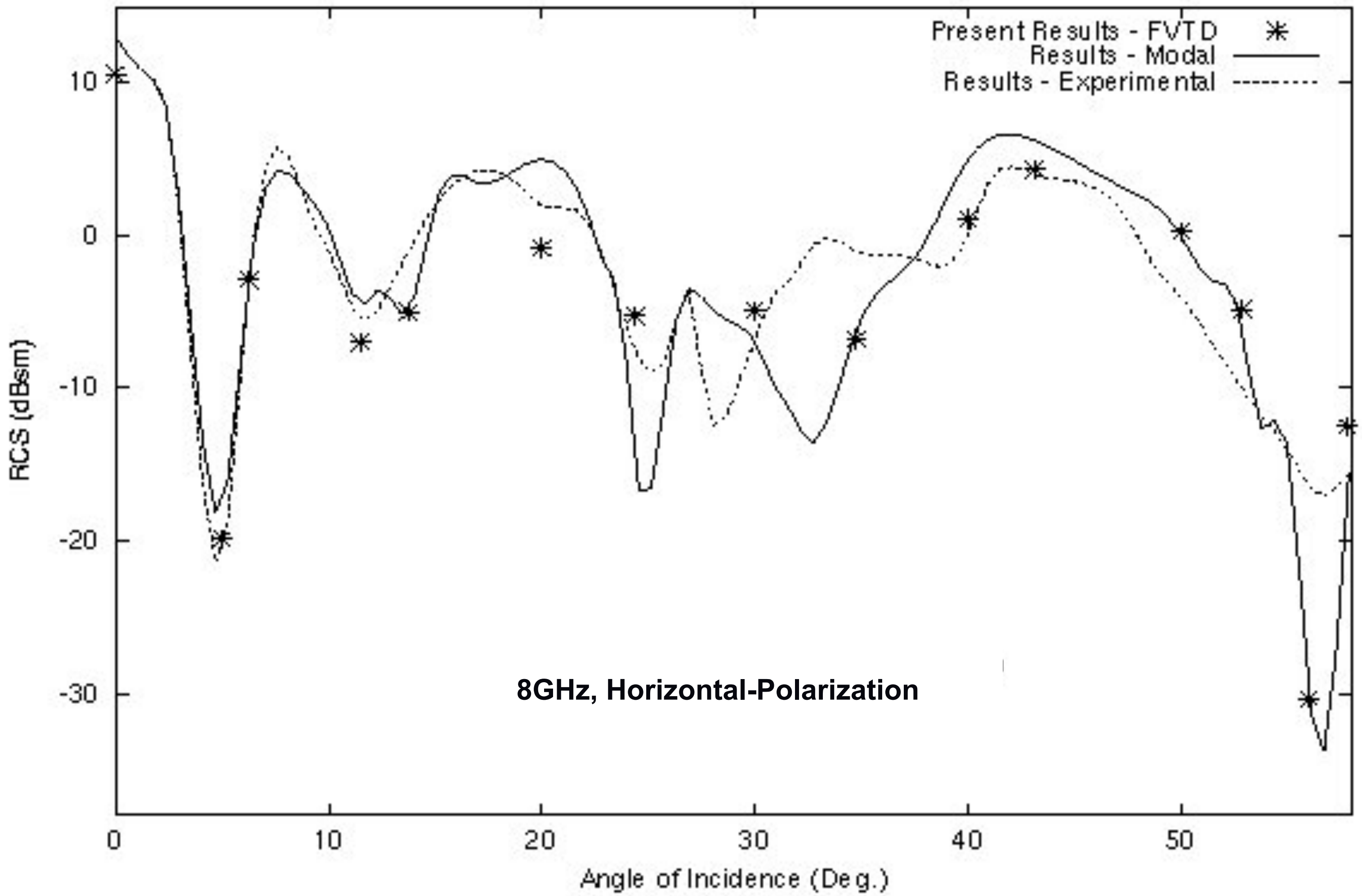

Monostatic RCS: Straight Cylindrical Cavity with a Hub, Blades and Plate termination

RCS of some military aircrafts

Aircraft	RCS [dBsm]	RCS [m^2]	RCS [ft^2]
F-15 Eagle	26	405	4,358
F-4 Phantom II	20	100	1,076
B-52 Stratofortress	20	99.5	1,071
Su-27	12	15	161.4
B-1A	10	10	107.6
F-16 Fighting Falcon	7	5	53.82
B-1B Lancer	0.09	1.02	10.98
F-18E/F Super Hornet	0	1	10.76
BGM-109 Tomahawk	-13	0.05	0.538
SR-71 Blackbird	-18.5	0.014	0.15
F-22 Raptor	-22	0.0065	0.07
F-117 Nighthawk	-25	0.003	0.03
B-2 Spirit	-40	0.0001	0.01
Boeing Bird of Prey	-70	0.0000001	0.000008

Clean aircraft configurations

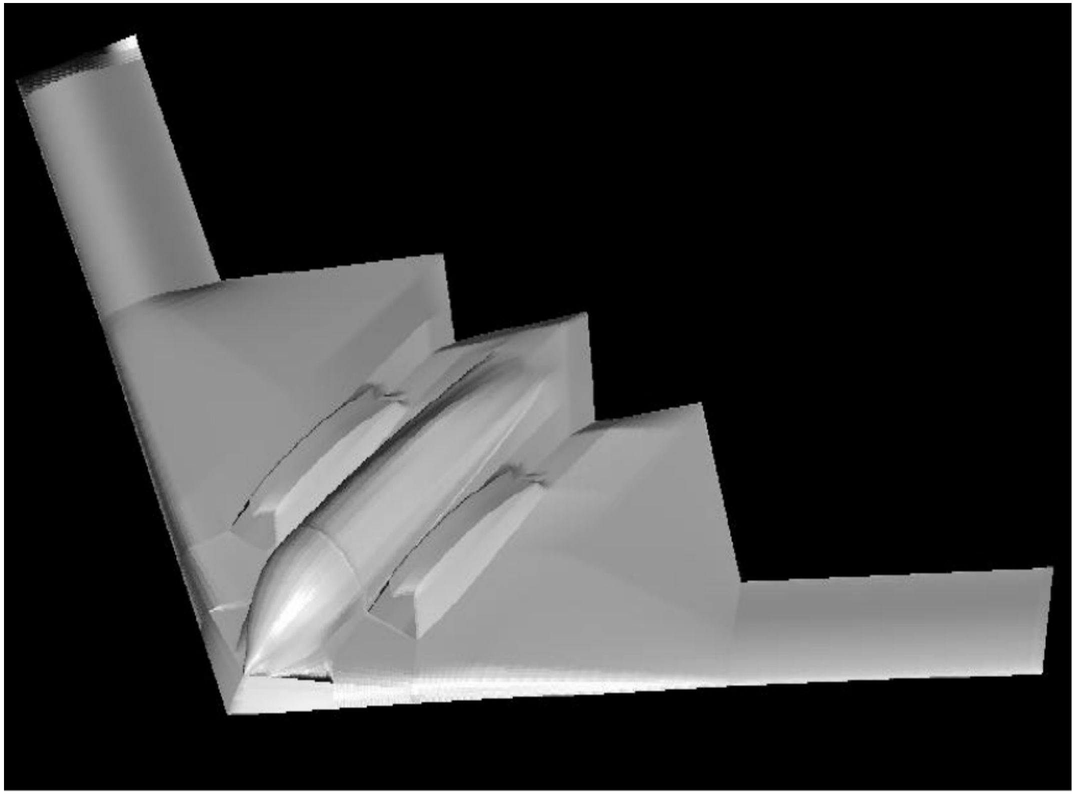

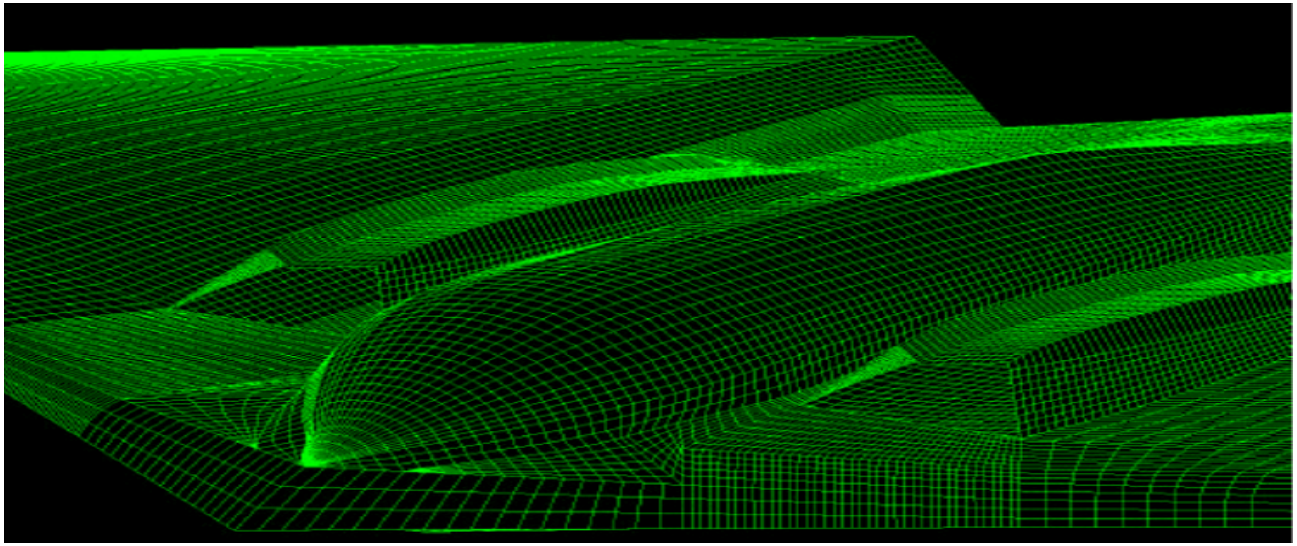

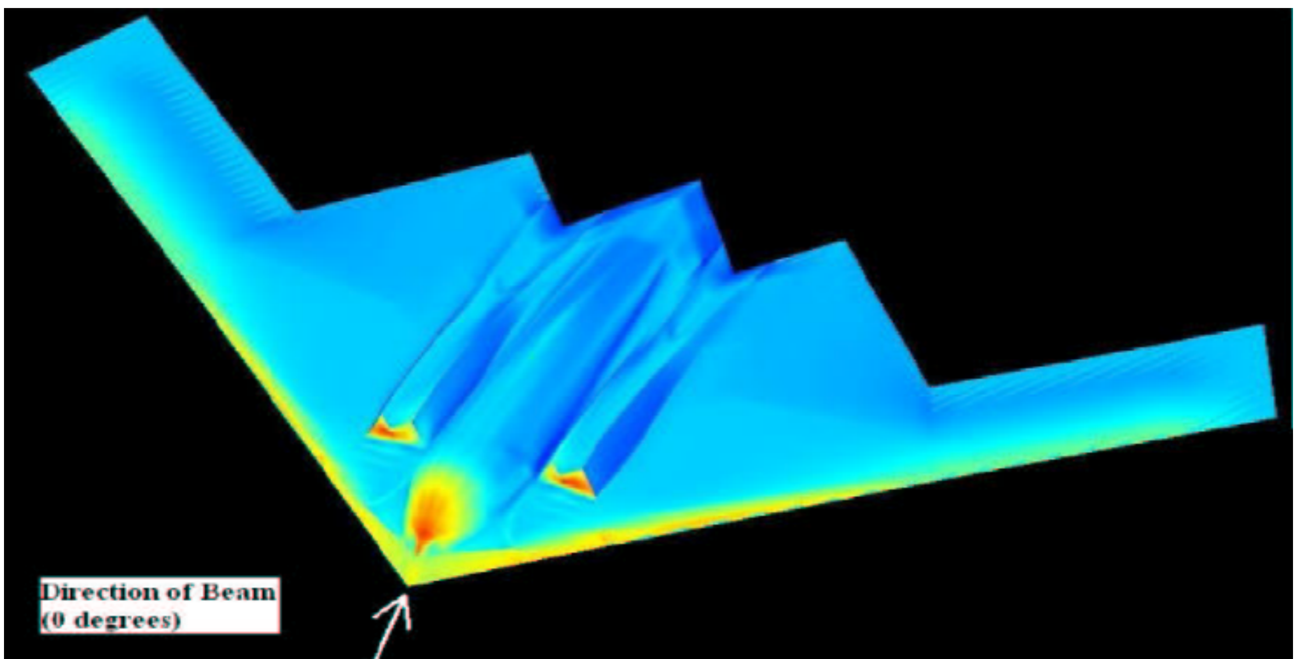
Direction of Beam
(0 degrees)

Clean aircraft configurations

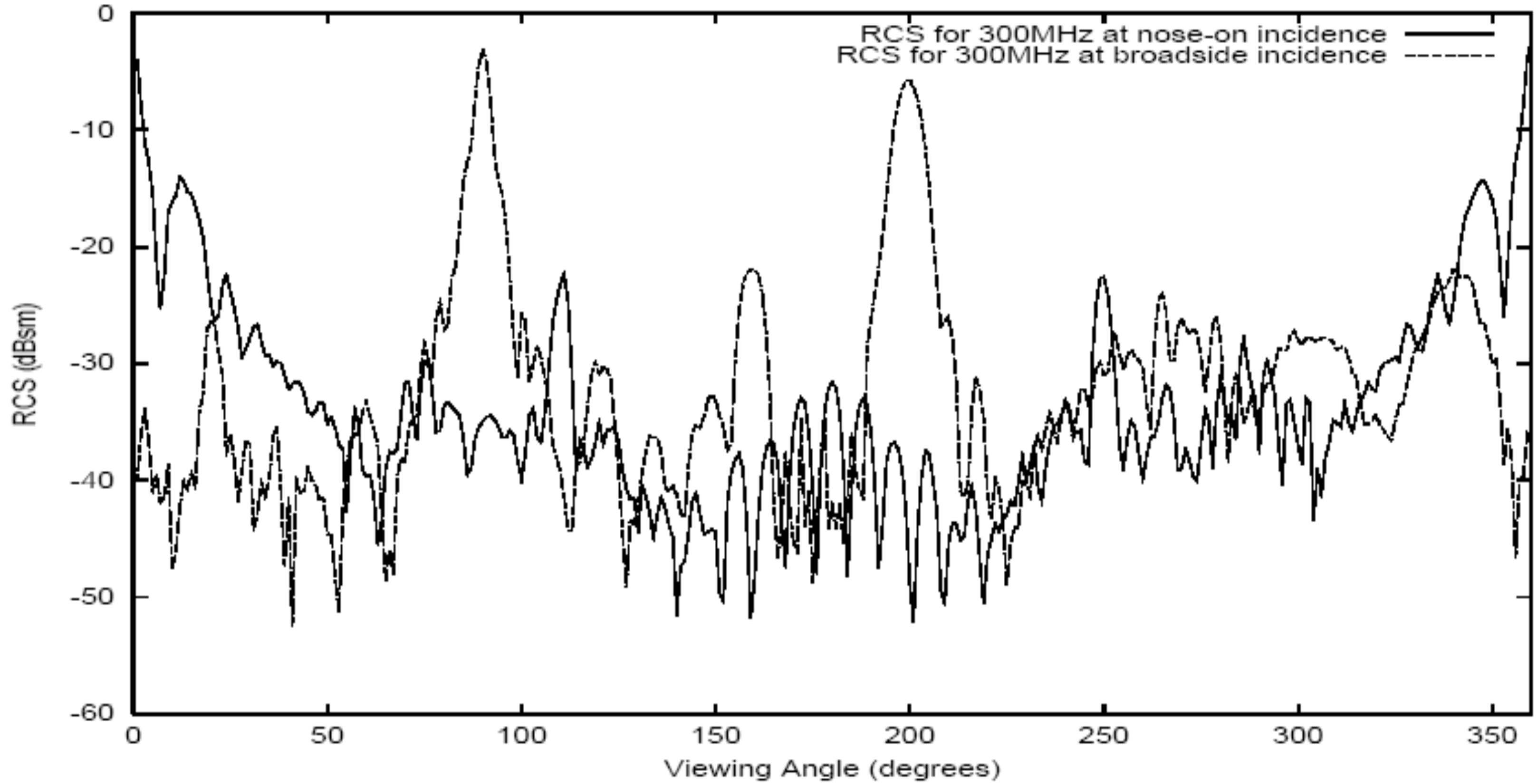

Bistatic RCS for 300 MHz (VV polarization) (Back-scatter at 180 degrees for nose-on and 270 degrees for broadside incidences)

Bi-static RCS Plot @ 300 MHz (VV)

VFY218 in literature

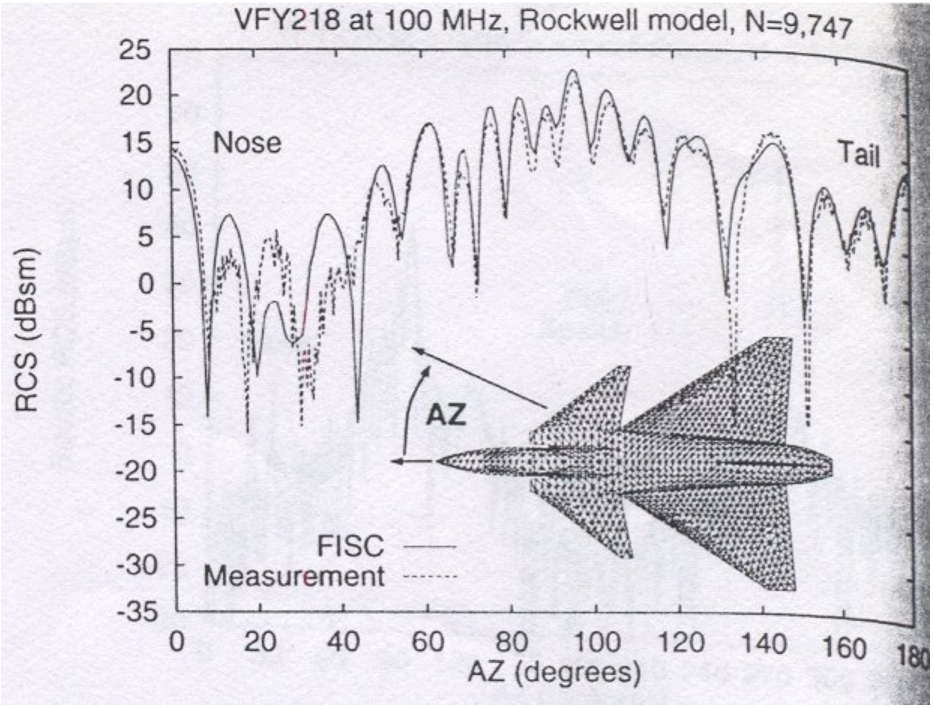

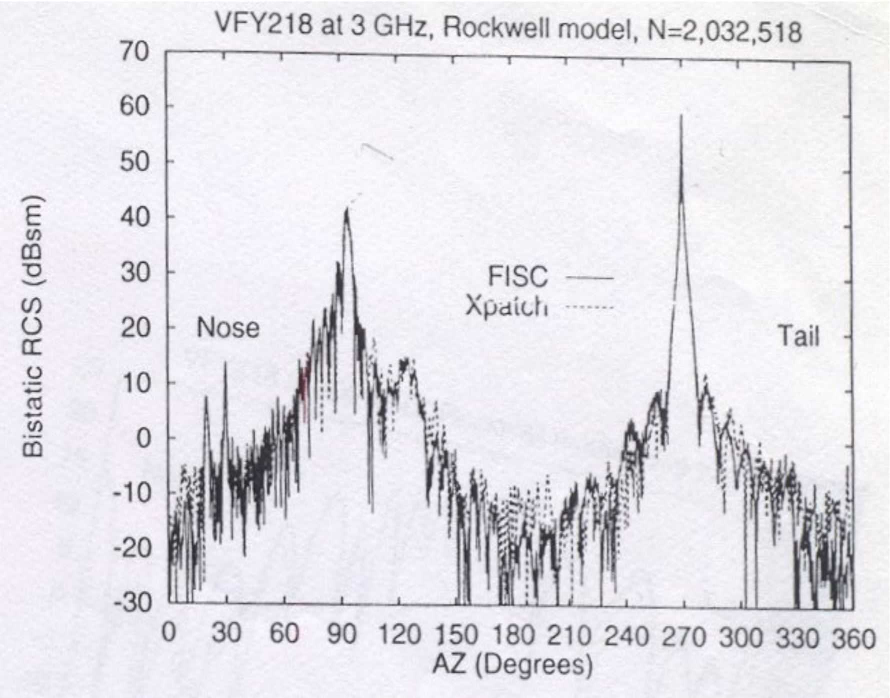

100MHz, Nose-on Incidence, monostatic

2GHz, Side-on Incidence, bi

Clean aircraft configurations

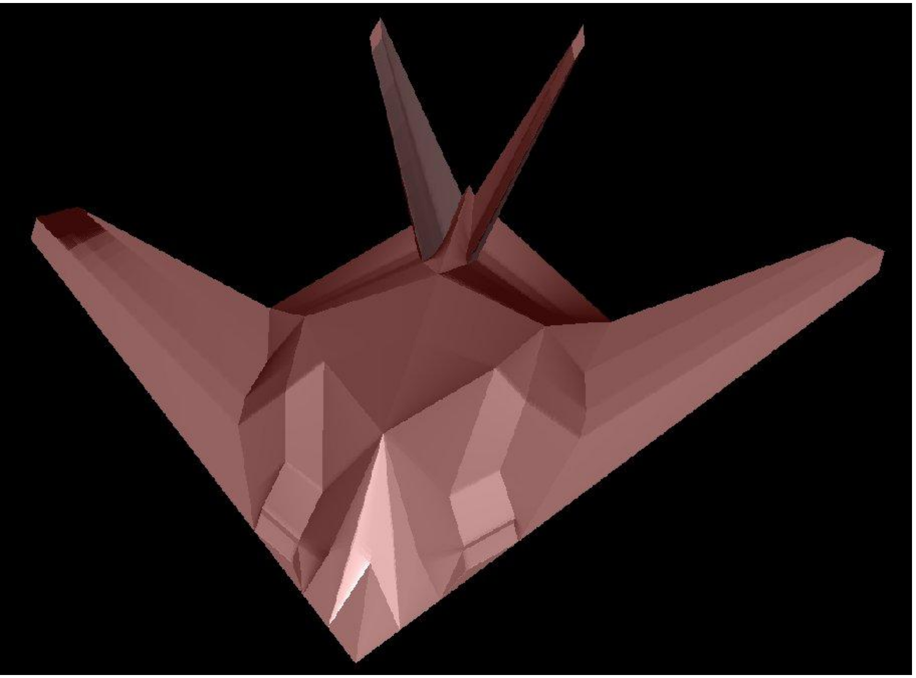

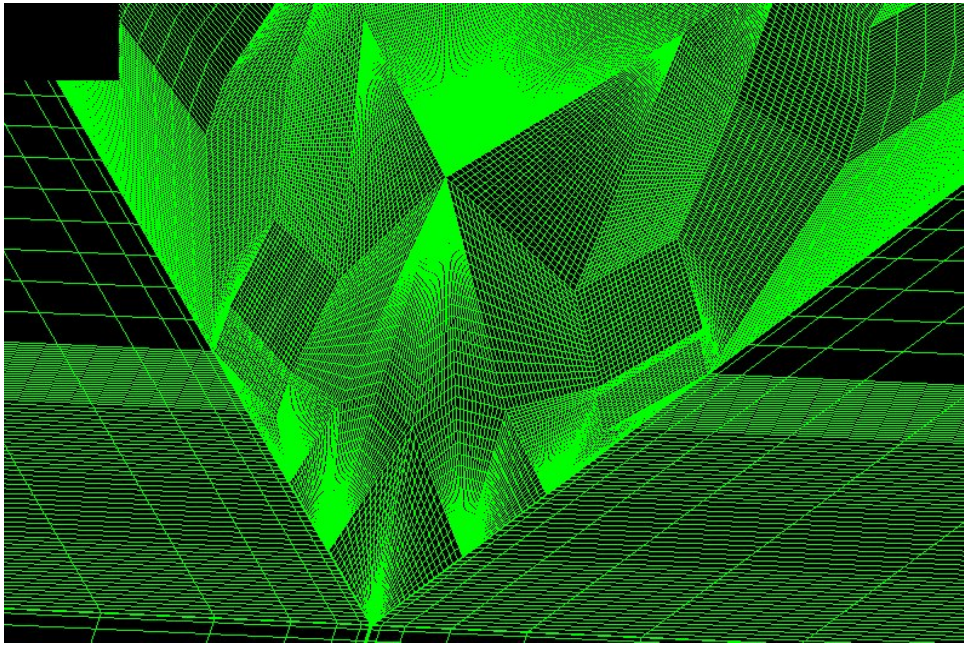

Rendered Image of Surface Grid

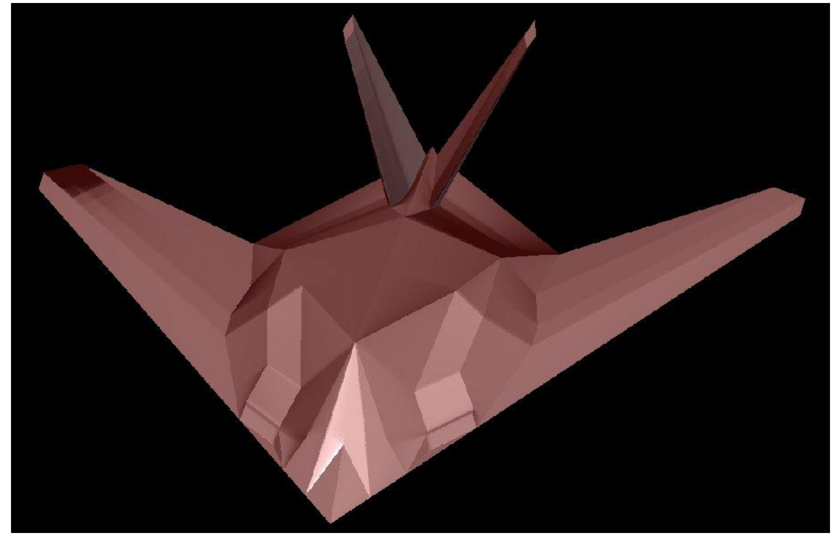

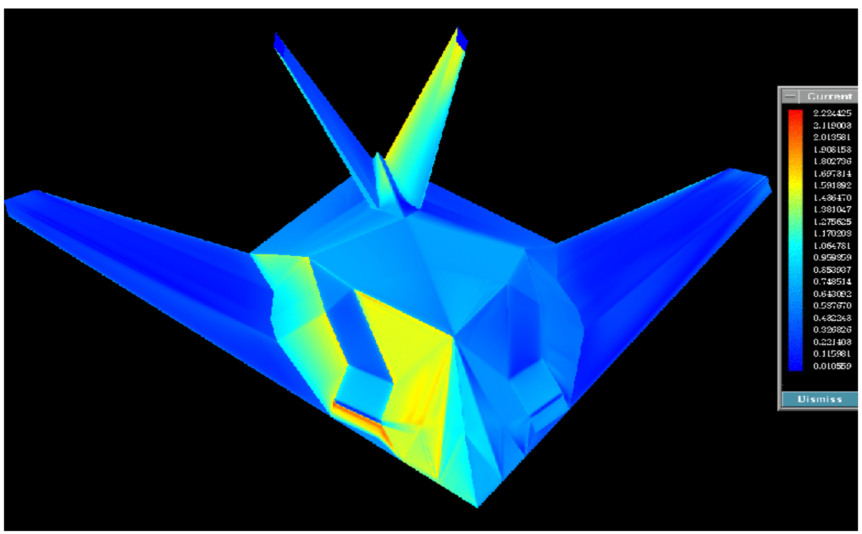
Current
2.224425
2.119003
2.013581
1.908158
1.802736
1.697314
1.591892
1.486470
1.381047
1.275625
1.170203
1.064781
0.959359
0.853937
0.748514
0.643092
0.537670
0.432248
0.326826
0.221403
0.115981
0.010559
Dismiss

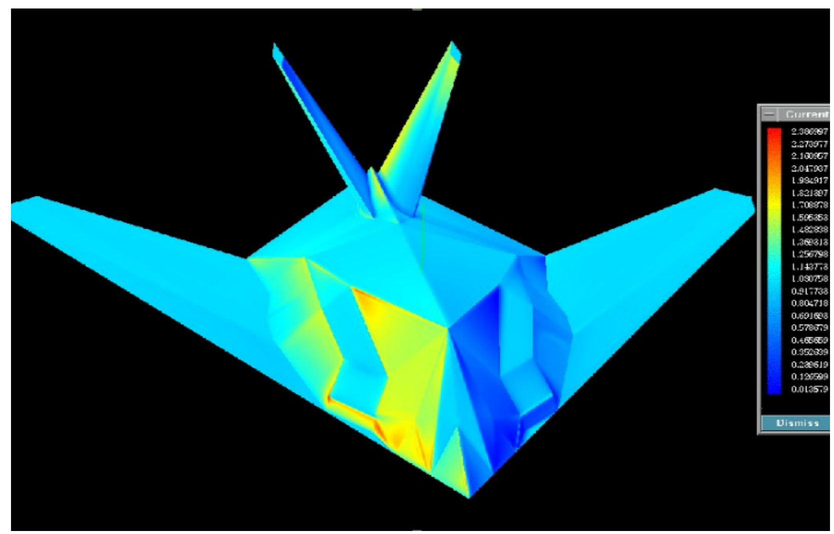
Current
Dismiss

Clean aircraft configuration

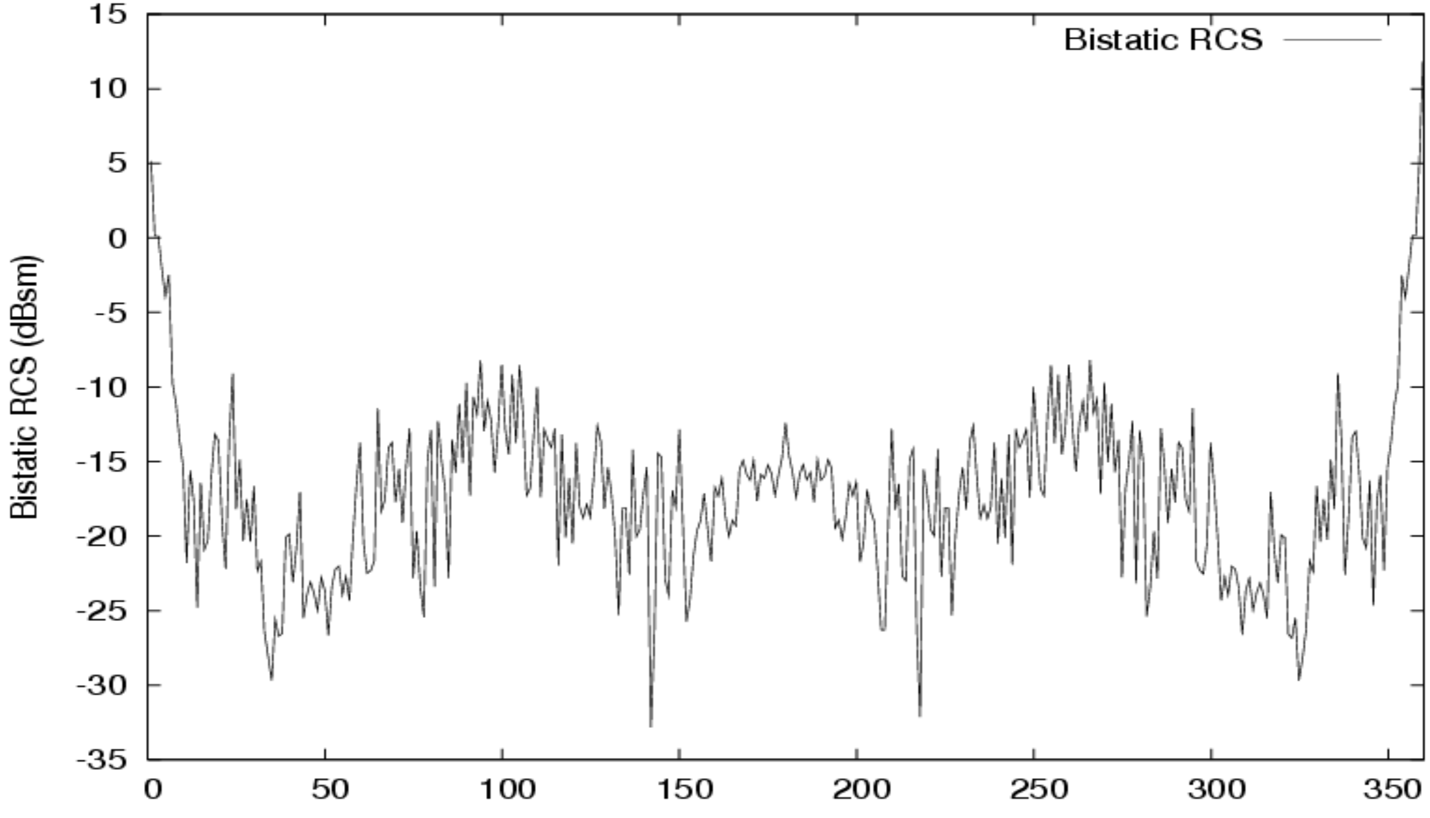

Bi-static RCS Plot @ 280 MHz (VV)

The unstructured approa

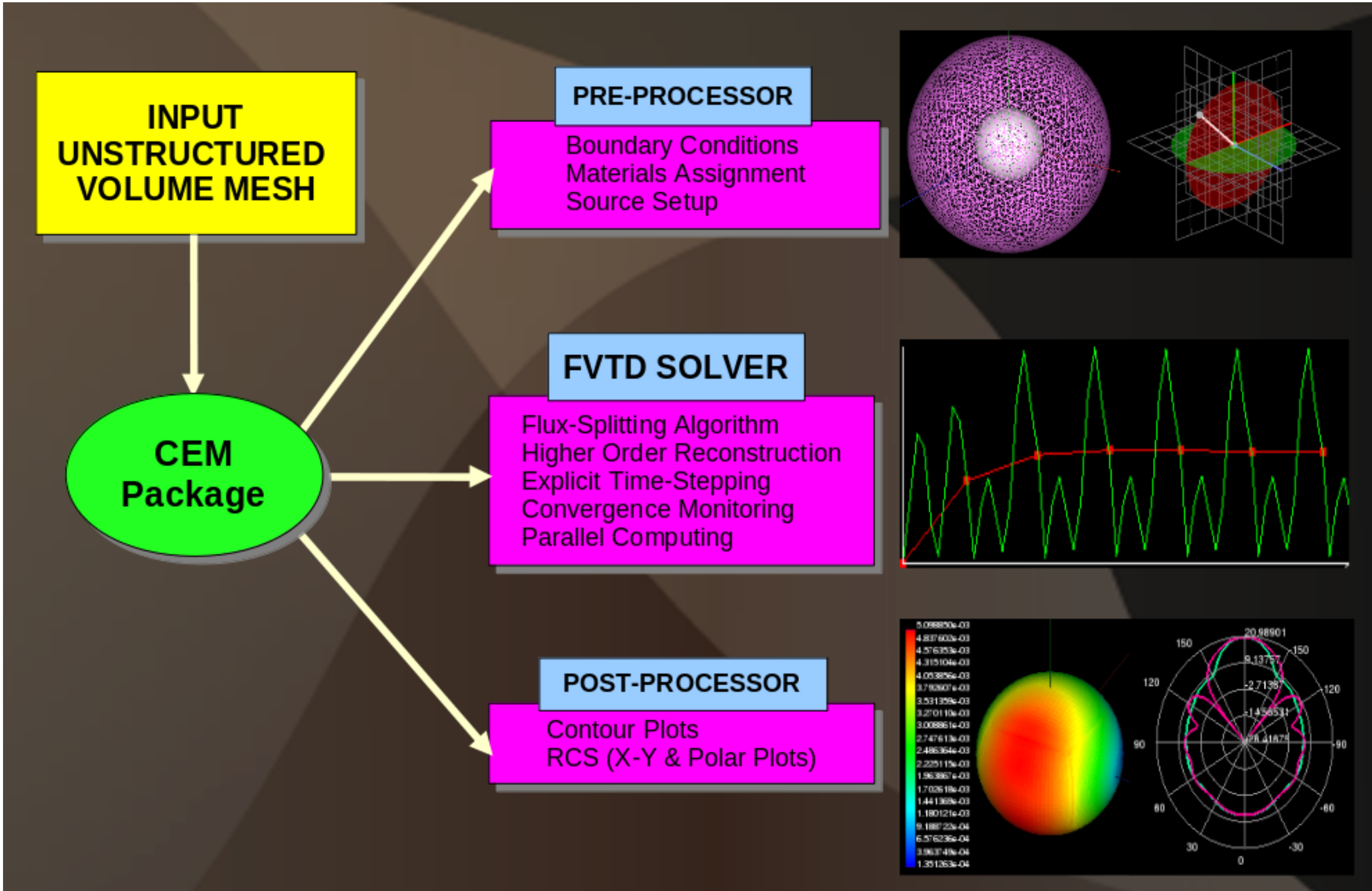

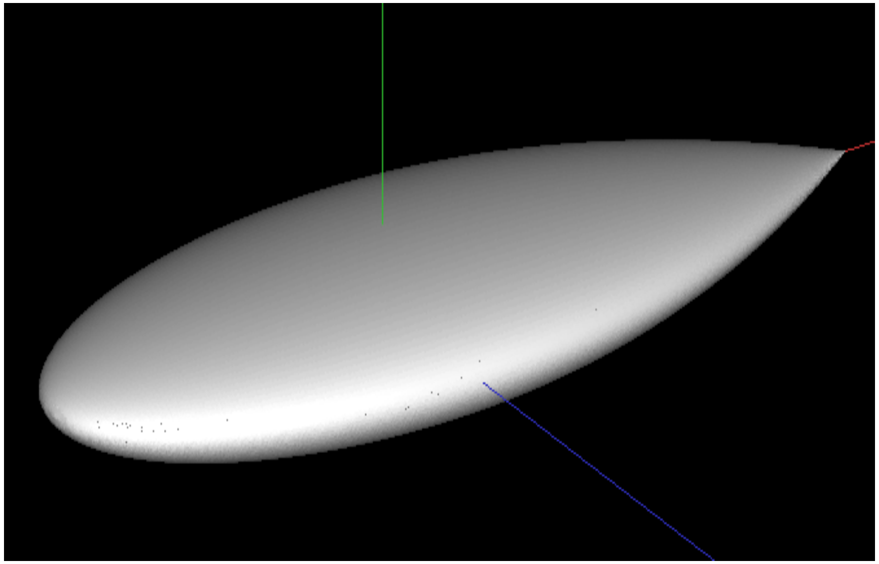

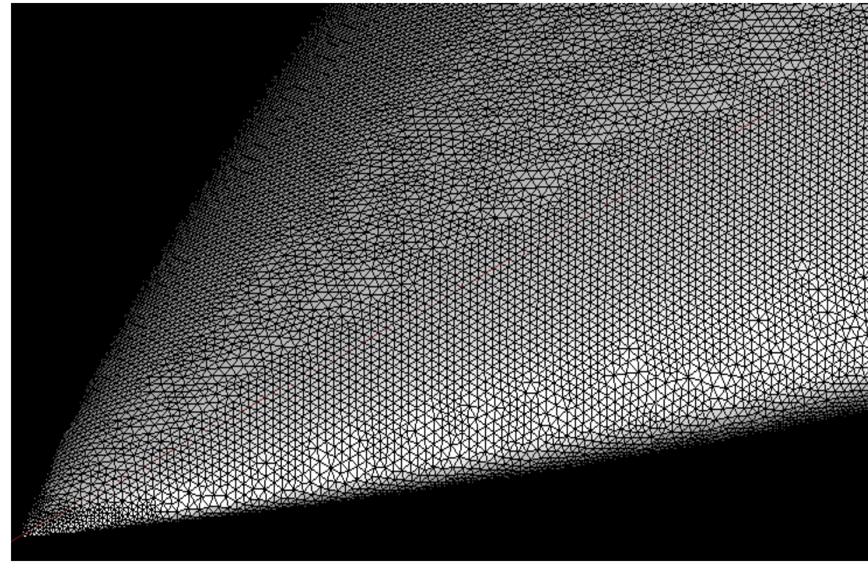

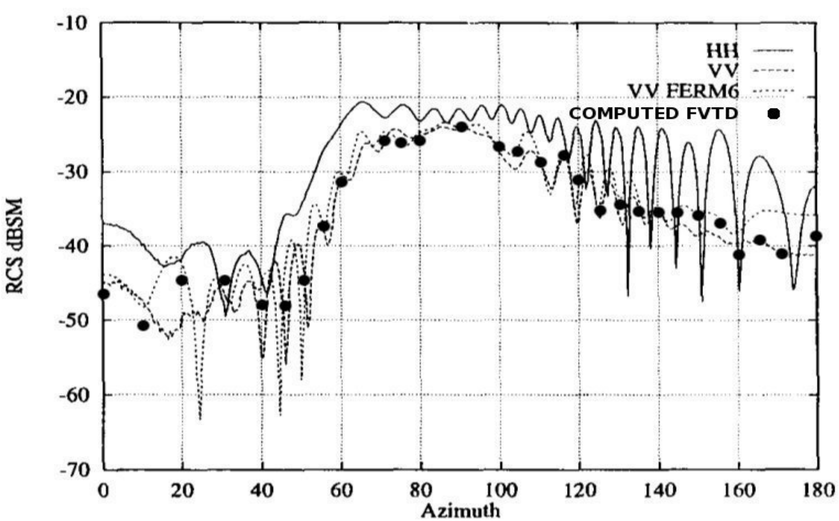
-10
-20
-30
-40
-50
-60
-70
RCS dBSM
0
20
40
60
80
100
120
140
160
180
Azimuth
HH
VV
VV FERM6
COMPUTED FVTD

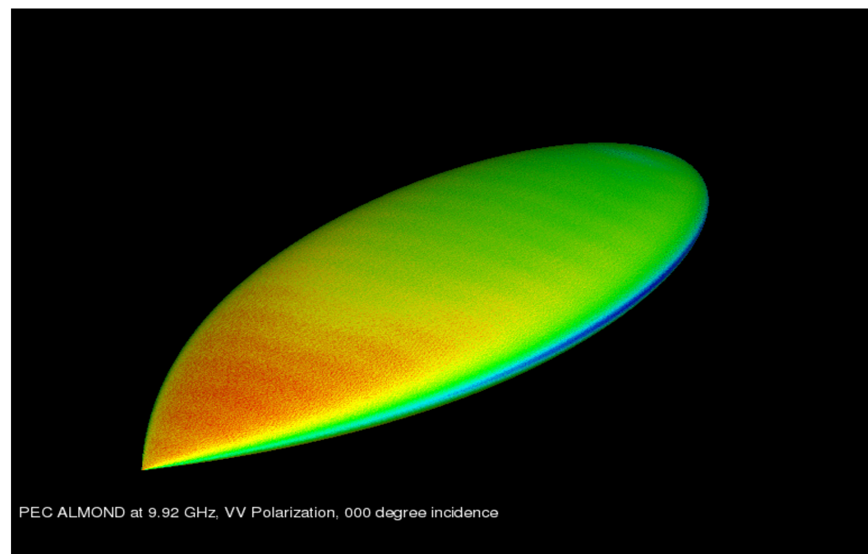
PEC ALMOND at 9.92 GHz, VV Polarization, 000 degree incidence

The unstructured approach - almond

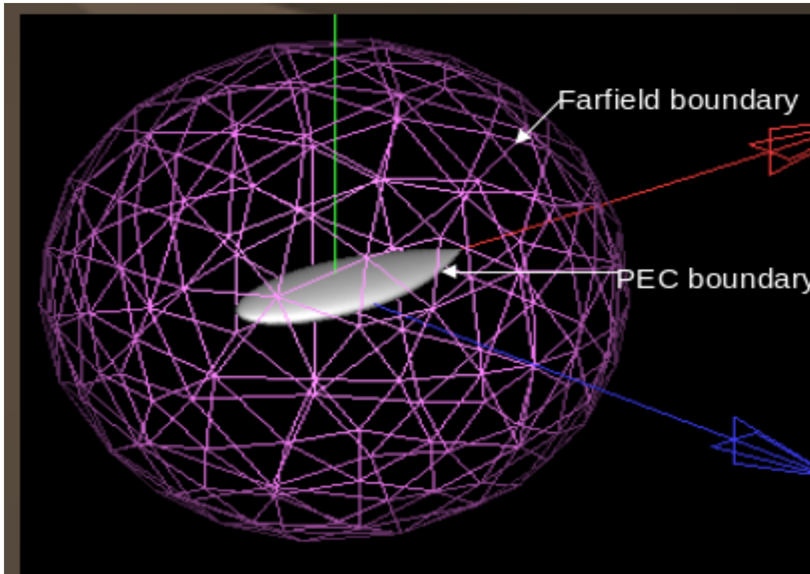

Boundary Conditions

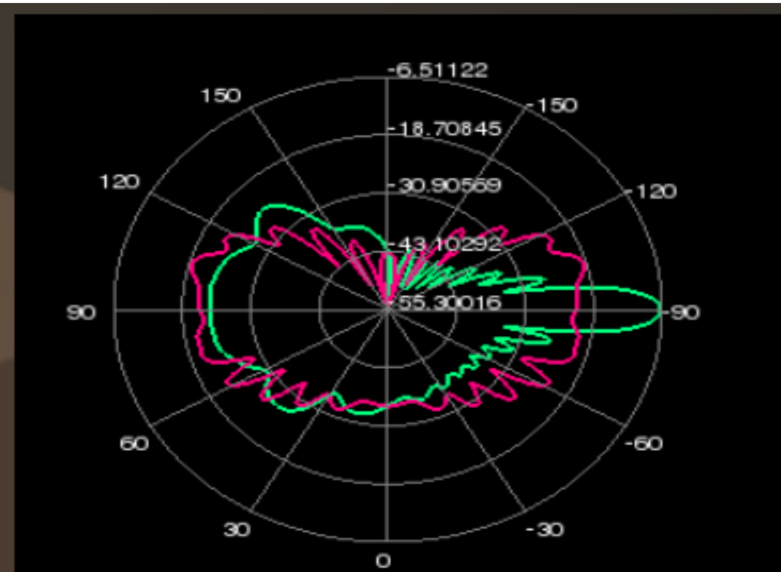

Bistatic RCS at 90 degree Incidence, E-H Plane

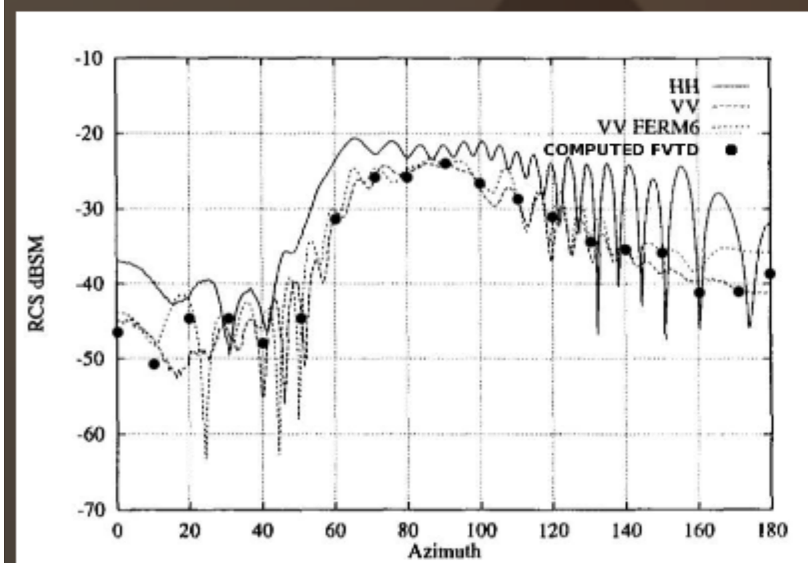

Monostatic RCS Comparison with Measurements

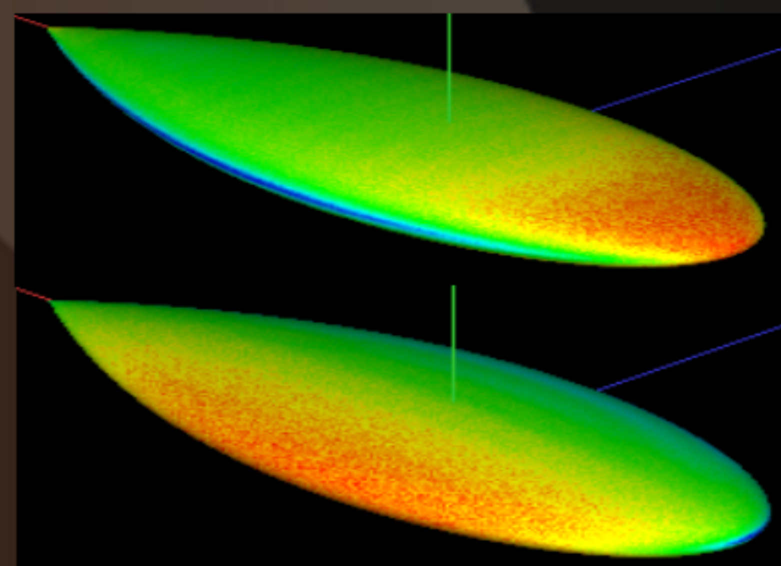
Surface Currents at 0 and 90 degree incidences

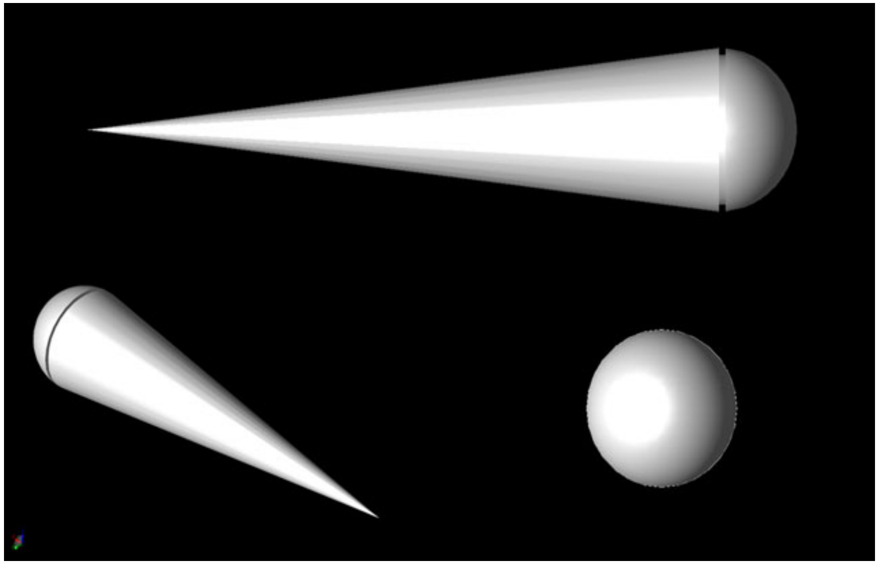

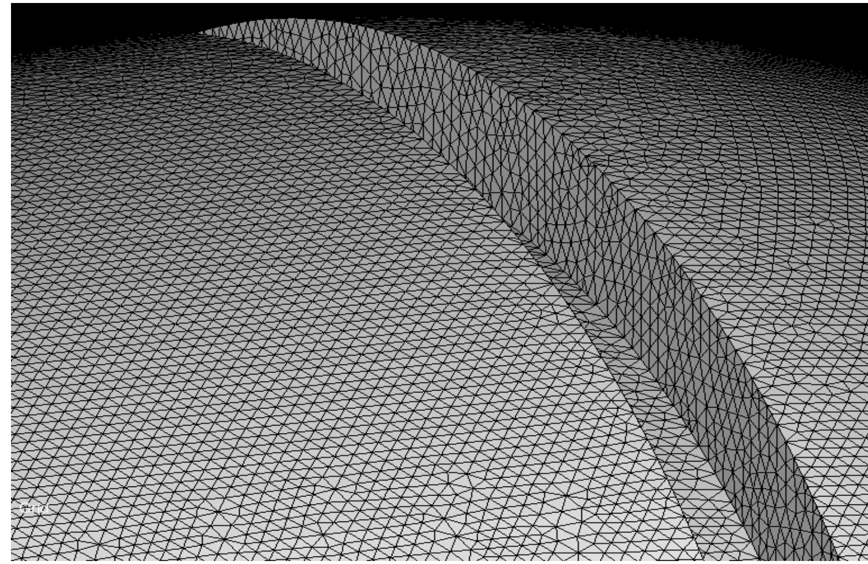

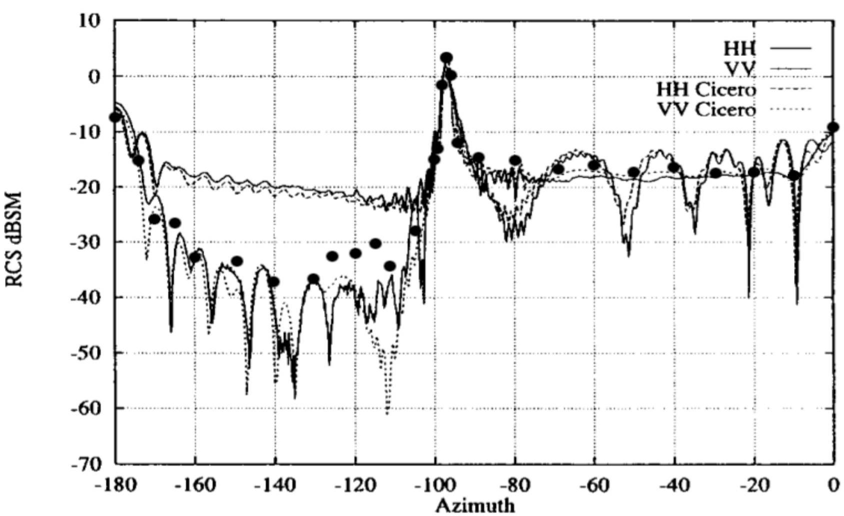

HH
VV
HH Cicero
VV Cicero
RCS dBSM
10
0
-10
-20
-30
-40
-50
-60
-70
-180
-160
-140
-120
-100
-80
-60
-40
-20
0
Azimuth

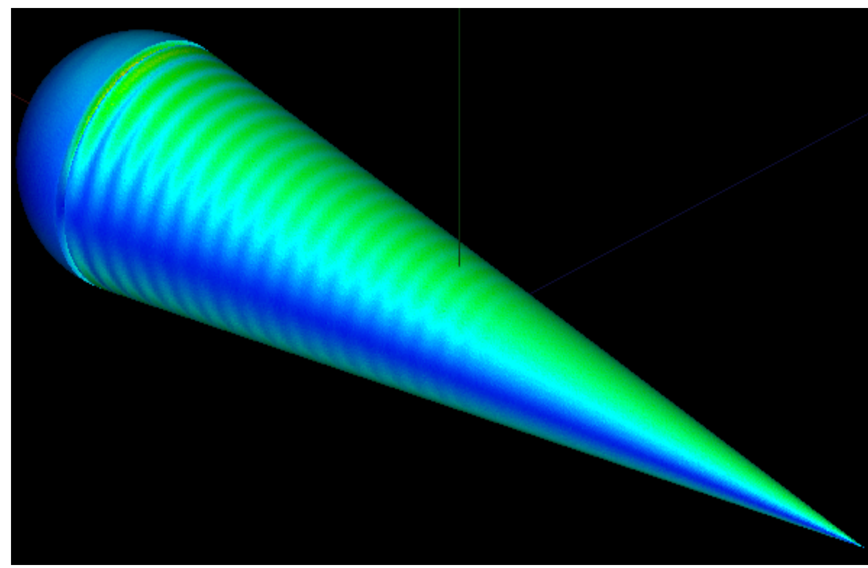

Cone-sphere with gap

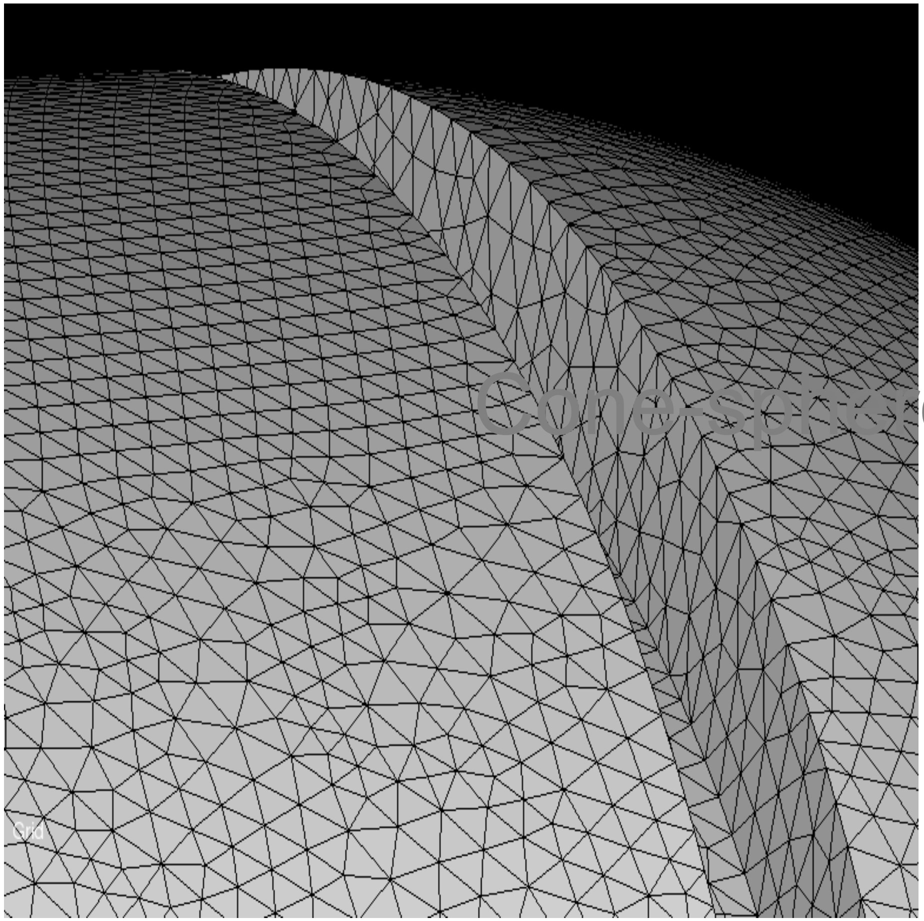

rface mesh for 869 MHz frequency

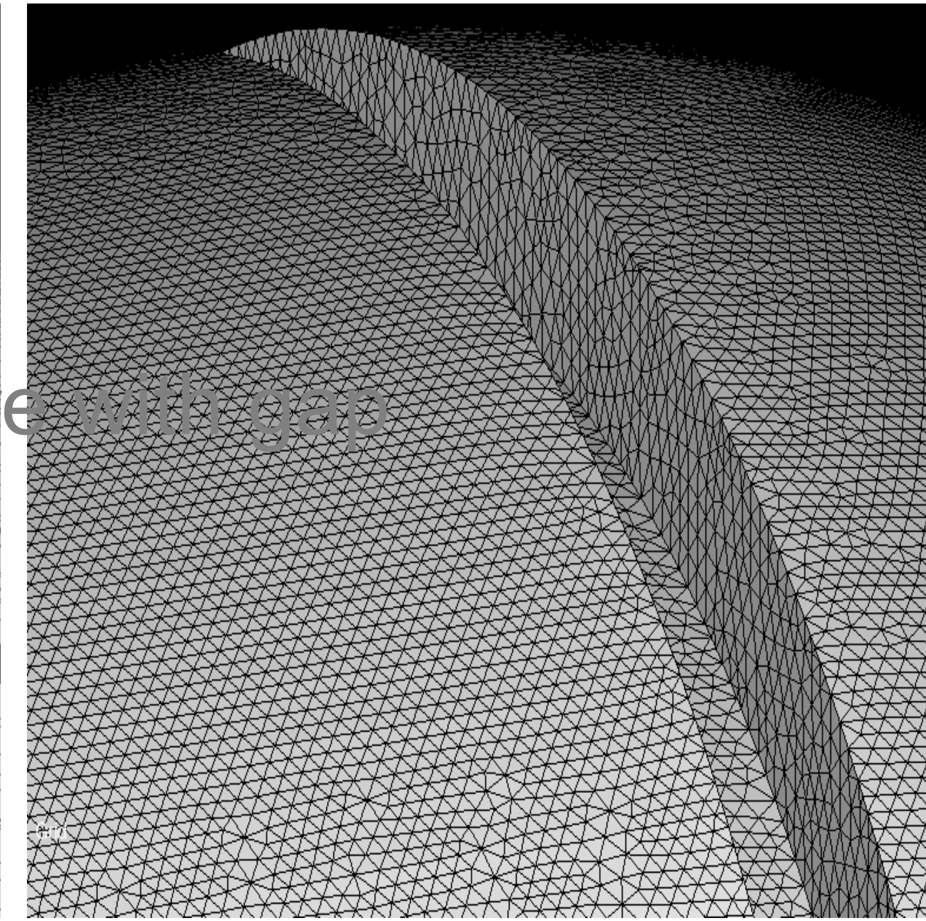

Surface mesh for 9 GHz fr

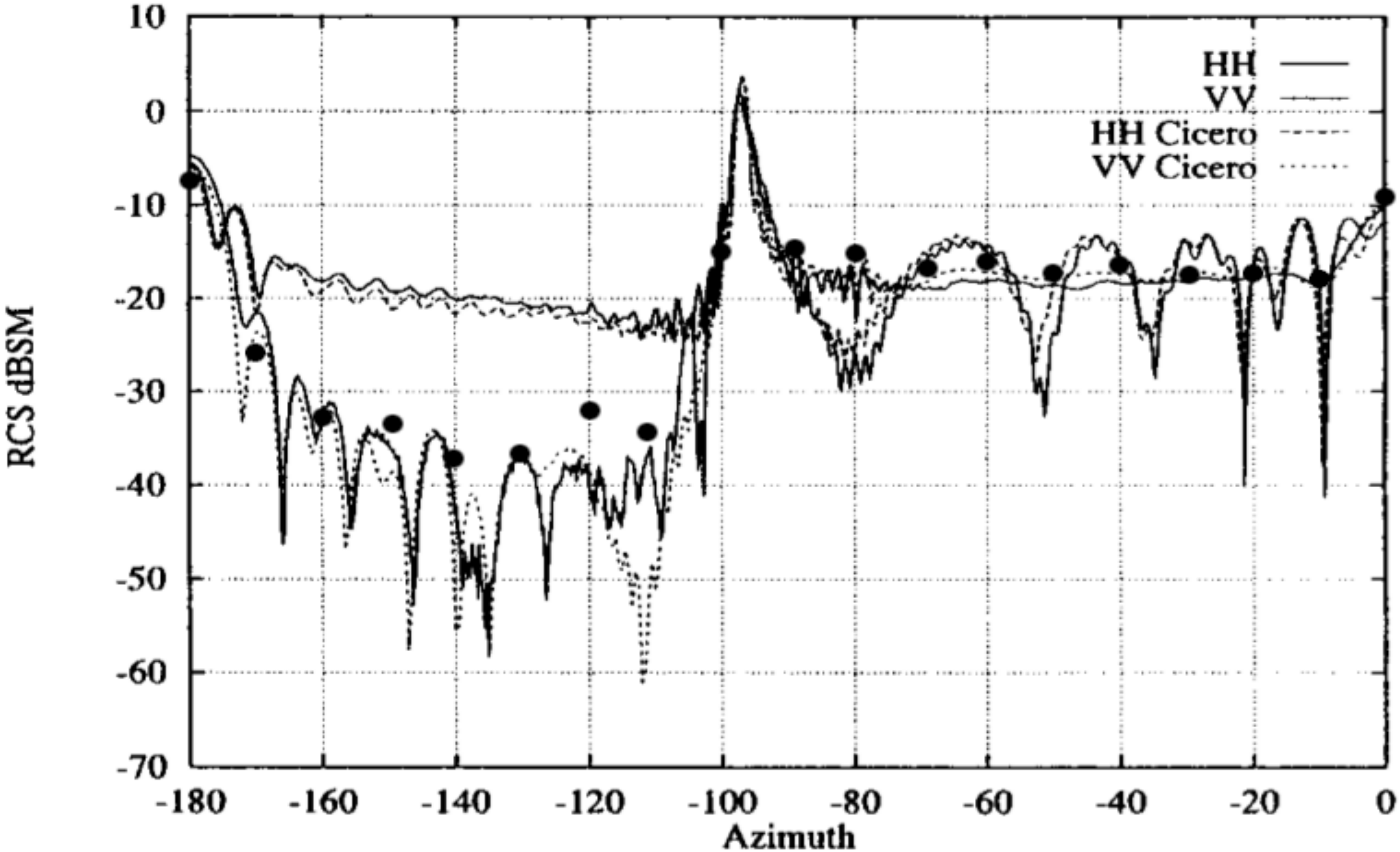

Computed Monostatic RCS for Cone-sphere with gap

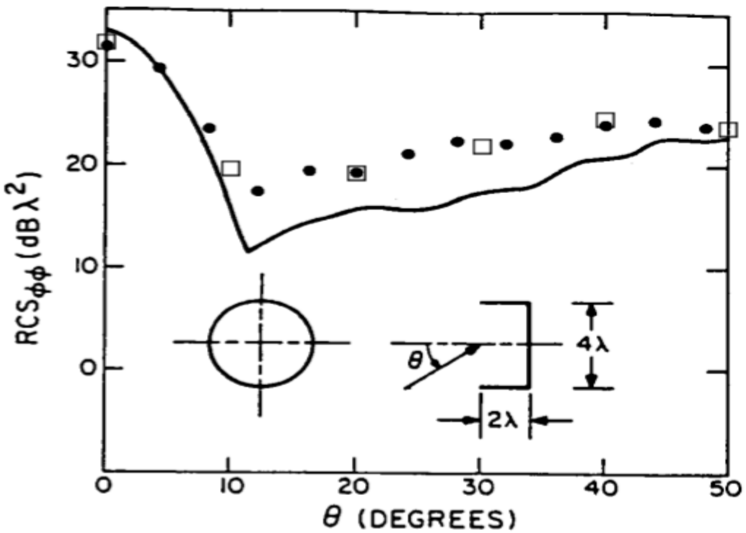

RCSφφ (dBλ²)
θ (DEGREES)
4λ
2λ
θ
0 10 20 30 40 50
30 20 10 0

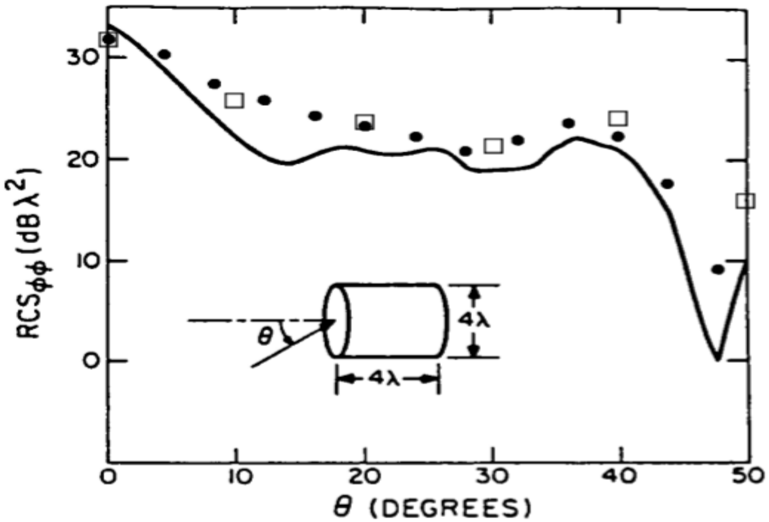

RCSφφ (dBλ²)
θ (DEGREES)
4λ
4λ
θ
0 10 20 30 40 50
30 20 10 0

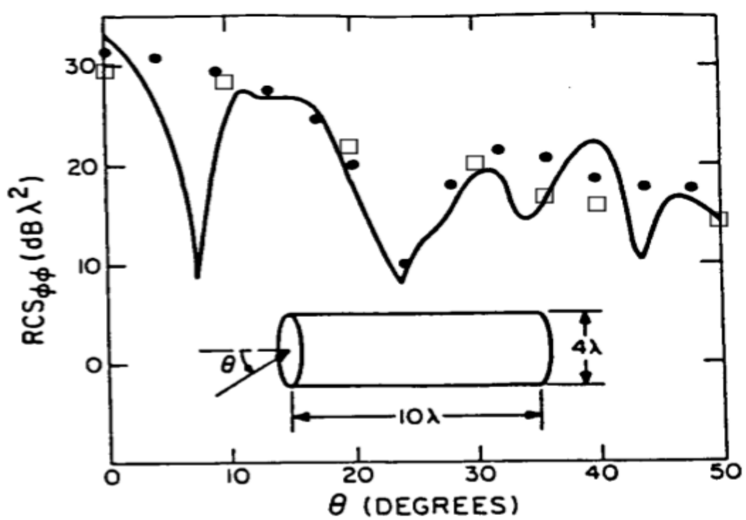

RCSφφ (dBλ²)
θ (DEGREES)
4λ
10λ
θ
0 10 20 30 40 50
30 20 10 0

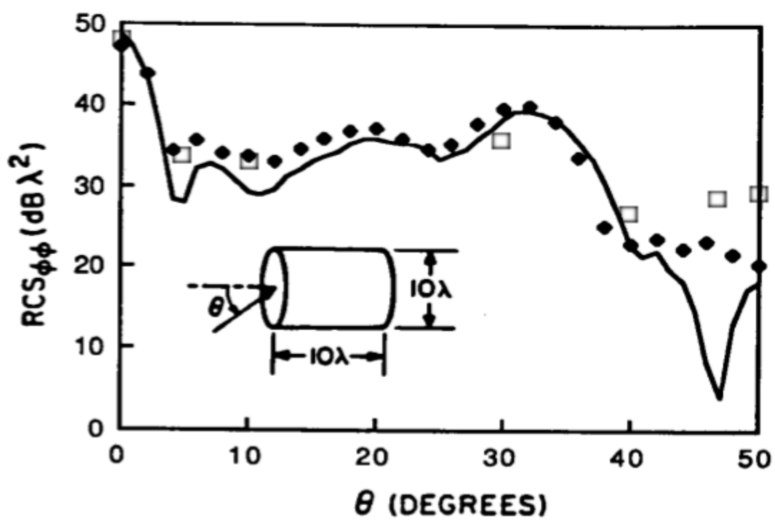

RCSφφ (dBλ²)
θ (DEGREES)
10λ
10λ
θ
0 10 20 30 40 50
50 40 30 20 10 0

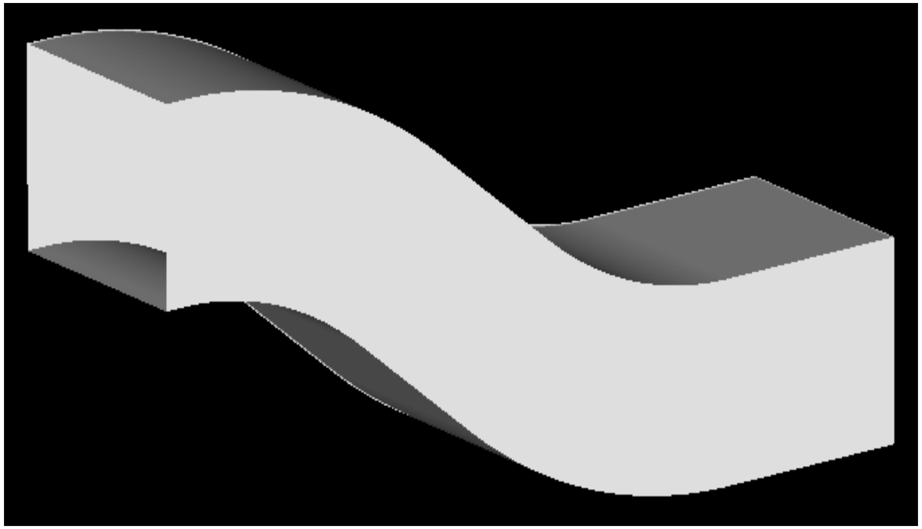

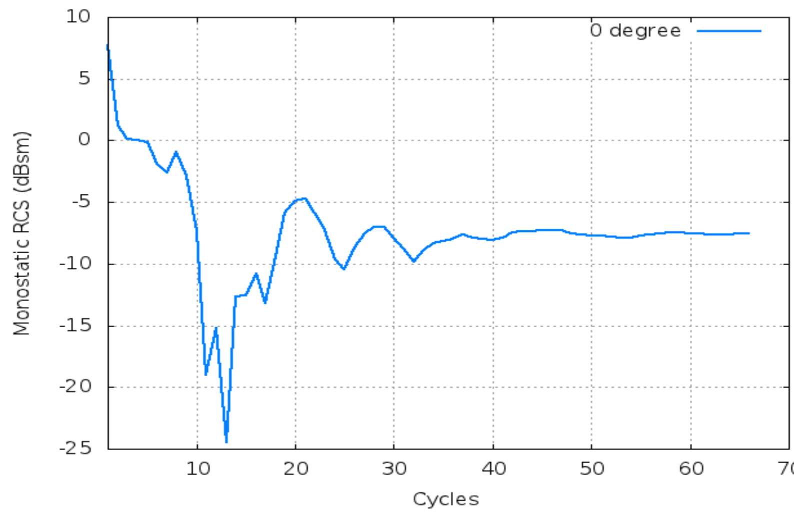
0 degree
Monostatic RCS (dBsm)
Cycles
10
5
0
-5
-10
-15
-20
-25
10
20
30
40
50
60
70

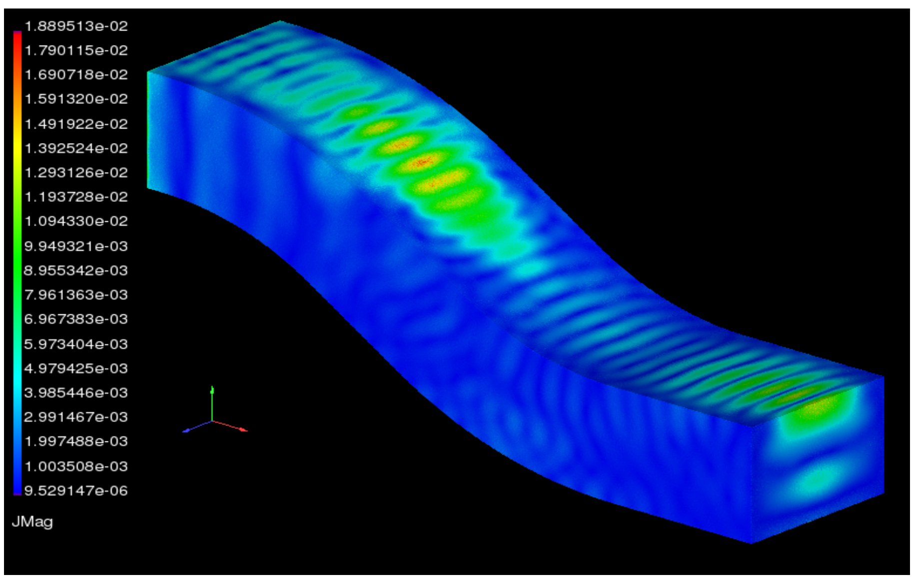
1.889513e-02
1.790115e-02
1.690718e-02
1.591320e-02
1.491922e-02
1.392524e-02
1.293126e-02
1.193728e-02
1.094330e-02
9.949321e-03
8.955342e-03
7.961363e-03
6.967383e-03
5.973404e-03
4.979425e-03
3.985446e-03
2.991467e-03
1.997488e-03
1.003508e-03
9.529147e-06
JMag

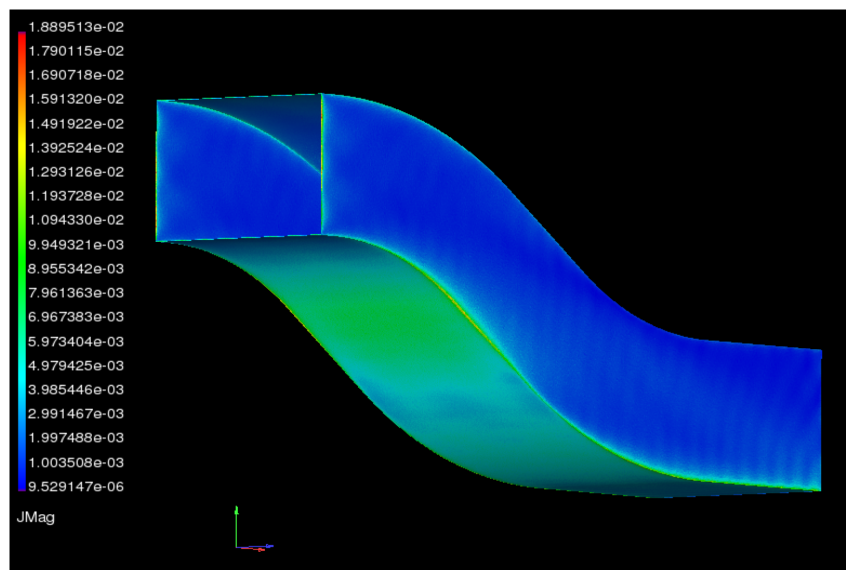
1.889513e-02
1.790115e-02
1.690718e-02
1.591320e-02
1.491922e-02
1.392524e-02
1.293126e-02
1.193728e-02
1.094330e-02
9.949321e-03
8.955342e-03
7.961363e-03
6.967383e-03
5.973404e-03
4.979425e-03
3.985446e-03
2.991467e-03
1.997488e-03
1.003508e-03
9.529147e-06
JMag

Metallic sphere coated with lossy dielectric

- PEC ka = 1.5
- Coating (t / λ) = 0.05, ε_r = 3.0 – j4.0, μ_r = 5.0 – j6.0
- Volume Grid O-O Topology, Single Block (64×48×32 cells)

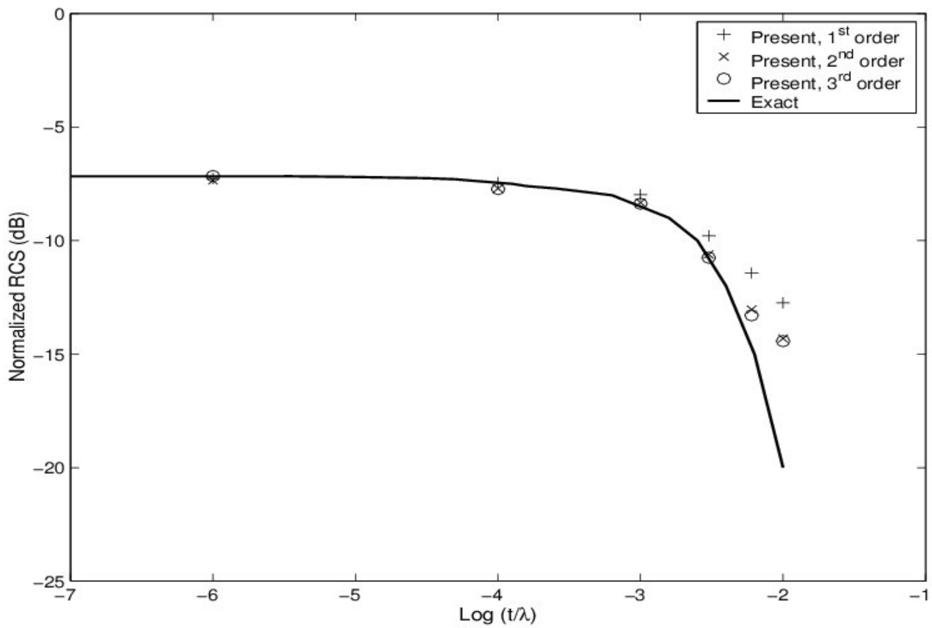

For different orders of accuracy

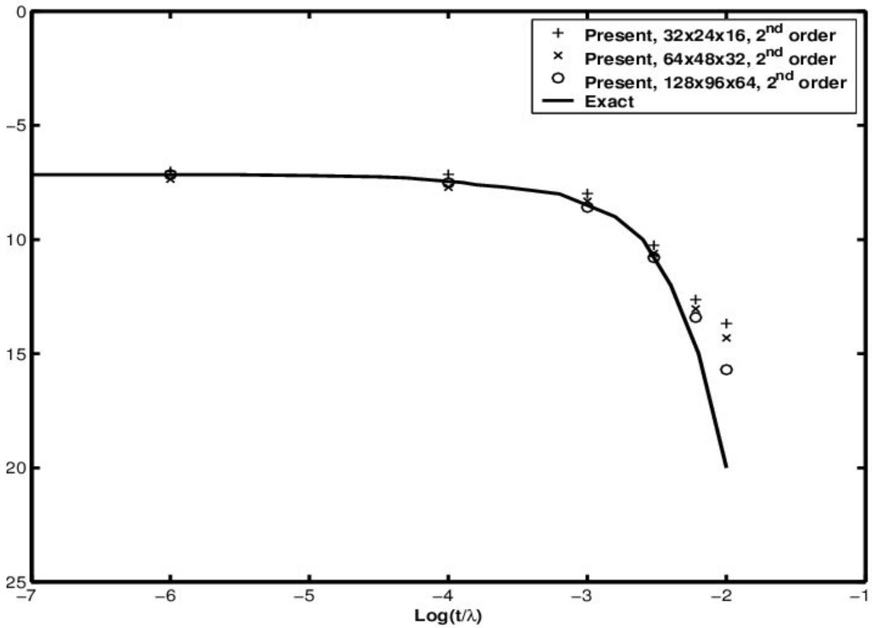

For different discretization

Monostatic RCS Sphere with Lossy Coating

EM wave propagation – complex media

- EM wave propagation in linearly dispersive media (Debye, Lorentz dielectric….)
- Models water, ice, tissues, muscle, RAM
- Application in EM interrogation of tissues like microwave imaging for breast cancer detection, effects of radiation exposure etc.
- Auxiliary Differential Equations solved for updating polarization vector in Ampere's law for M-pole Debye (water based) medium.

Pulsed wave propagation – linearly dispersive media

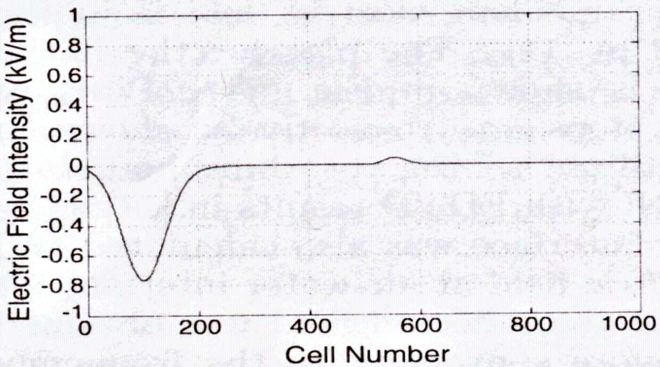

Figure 3. Total electric field after 1200 time steps.

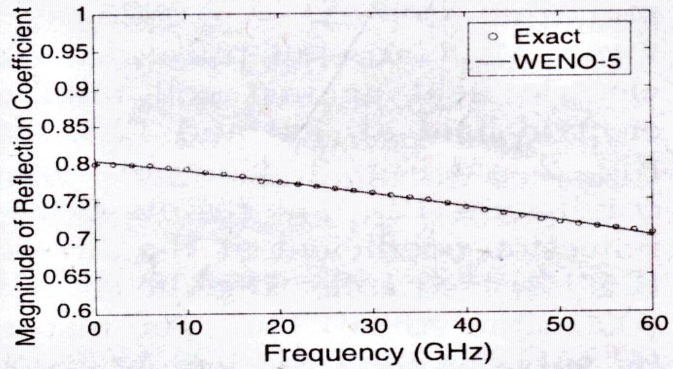

Figure 4. Computed magnitude of reflection coefficient at air-water interface compared with exact results.

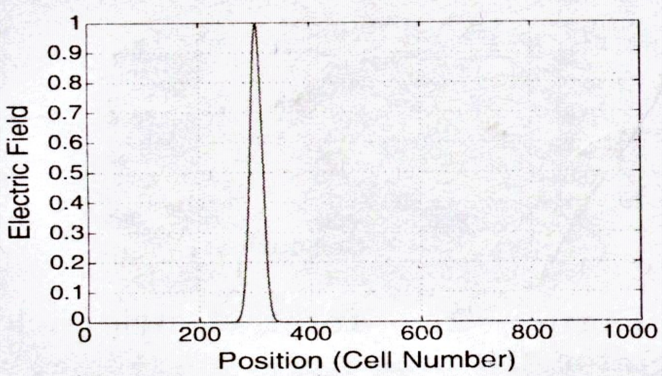

Figure 5. Initial electric field.

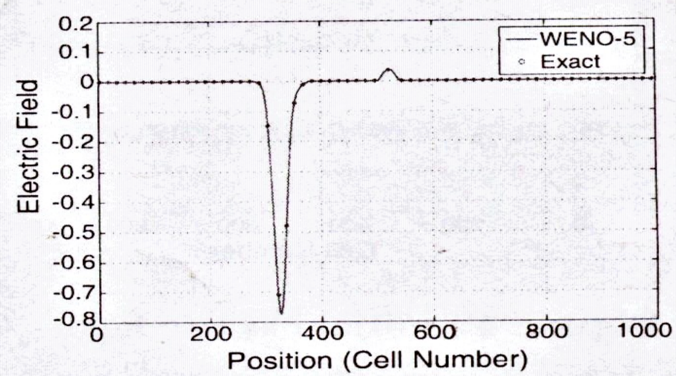

Figure 6. The exact and computed and electric field after 750 time steps.

Single pole (*water*) and five pole *(muscle)* Debye dielectric, *Journal Electromagnetic Waves & Applications 2009.*

Applications

- Helicopters
- KFX
- LCA, UCAV, AMCA